

# Rigorous numerics in Floquet theory: computing stable and unstable bundles of periodic orbits

Roberto Castelli \*

Jean-Philippe Lessard<sup>†</sup>

## Abstract

In this paper, a rigorous method to compute Floquet normal forms of fundamental matrix solutions of non-autonomous linear differential equations with periodic coefficients is introduced. The Floquet normal form of a fundamental matrix solution  $\Phi(t)$  is a canonical decomposition of the form  $\Phi(t) = Q(t)e^{Rt}$ , where  $Q(t)$  is a real periodic matrix and  $R$  is a constant matrix. To compute rigorously the Floquet normal form, the idea is to use the regularity of  $Q(t)$  and to solve simultaneously for  $R$  and  $Q(t)$  with the contraction mapping theorem in a Banach space of rapidly decaying coefficients. The explicit knowledge of  $R$  and  $Q$  can then be used to construct, in a rigorous computer-assisted way, stable and unstable bundles of periodic orbits of vector fields.

## Keywords

Rigorous numerics · Floquet theory · Fundamental matrix solutions · Contraction mapping theorem · Periodic orbits · Tangent bundles

## Mathematics Subject Classification (2000)

37B55 · 37M99 · 37C27 · 65G99 · 34D05

## 1 Introduction

In his seminal work [1] of 1883, Gaston Floquet studied linear non-autonomous differential equations of the form

$$\dot{y} = A(t)y, \quad (1)$$

where  $A(t)$  is a  $\tau$ -periodic continuous matrix function of  $t$ . More precisely, Floquet introduces a canonical decomposition of the fundamental matrix solutions of (1).

**Theorem 1.1. [Floquet Theorem]** *Let  $A(t)$  be a  $\tau$ -periodic continuous matrix function and denote by  $\Phi(t)$  a fundamental matrix solution of (1). Then  $\Phi(t+\tau)$  is also a fundamental matrix solution,  $\Phi(t+\tau) = \Phi(t)\Phi^{-1}(0)\Phi(\tau)$ , and there exist a real constant matrix  $R$  and a real nonsingular, continuously differentiable,  $2\tau$ -periodic matrix function  $Q(t)$  such that*

$$\Phi(t) = Q(t)e^{Rt}. \quad (2)$$

---

\*BCAM - Basque Center for Applied Mathematics, Bizkaia Technology Park, 48160 Derio, Bizkaia, Spain.  
Phone: (+34) 946 567 842. Fax: (+34) 946 567 843. Email: [r.castelli@bcamath.org](mailto:r.castelli@bcamath.org).

<sup>†</sup>**Corresponding author.** Université Laval, Département de Mathématiques et de Statistique, Pavillon Alexandre-Vachon, 1045 avenue de la Médecine, Local 1056, Québec, (Québec), G1V 0A6, Canada and BCAM - Basque Center for Applied Mathematics, Bizkaia Technology Park, 48160 Derio, Bizkaia, Spain.  
Email: [jean-philippe.lessard@mat.ulaval.ca](mailto:jean-philippe.lessard@mat.ulaval.ca).

The proof can be found for instance in [2]. The decomposition (2) is called a *Floquet normal form* for the fundamental matrix solution  $\Phi(t)$ . The real time-dependent change of coordinates  $z = Q^{-1}(t)y$  transforms system (1) into a linear constant coefficients system of the form  $\dot{z} = Rz$ . A stability theorem demonstrates that the linear stability of the zero solution of (1) can be determined by the eigenvalues of the so-called *monodromy matrix*  $\Phi(\tau)$ . While there has been several methods to compute (even rigorously) fundamental matrix solutions of (1), we are not aware of any rigorous method to compute Floquet normal forms as introduced in Theorem 1.1. This is one of the goal of the present work.

The motivation for developing such computational method comes from the study of dynamical systems, where (1) arises naturally when studying linear stability of periodic solutions of vector fields  $\dot{y} = g(y)$ , where  $g : \mathbb{R}^n \rightarrow \mathbb{R}^n$  is a smooth map. Assume that  $\Gamma$  is a  $\tau$ -periodic orbit of  $\dot{y} = g(y)$  parameterized by  $\gamma(t) \in \mathbb{R}^n$  ( $t \in [0, \tau]$ ), and define the  $\tau$ -periodic matrix function  $A(t) = \nabla g(\gamma(t))$ , where  $\nabla g$  is the Jacobian matrix. Consider  $\Phi(t)$  the *principal* fundamental matrix solution of  $\dot{y} = A(t)y = \nabla g(\gamma(t))y$ , that is the unique fundamental matrix solution so that  $\Phi(0) = I$ , and assume that a Floquet normal form  $\Phi(t) = Q(t)e^{Rt}$  is known. The information from the Floquet normal form can be used to compute important dynamical properties of  $\Gamma$ : the linear stability of the periodic orbit  $\Gamma$  can be determined by the eigenvalues of  $R$  while the stable and unstable tangent bundles of  $\Gamma$  can be retrieved from the action of  $Q(t)$  (with  $t \in [0, \tau]$ ) on the eigenvectors of  $R$  (e.g. see Theorem 3.7). Also, using the parameterization method introduced in [3], the higher order terms of a parameterization of an orientable invariant manifold of a periodic orbit can be computed efficiently from the action of  $Q(t)$  on some given constant vectors. Therefore one motivation for developing computer-assisted proofs for Floquet normal forms is to compute rigorously high order parameterizations of invariant manifolds of periodic orbits.

Before proceeding further, let us mention that rigorous methods like the  $C^1$ -Lohner algorithm [4] can be used to study the linear stability of periodic orbits. For instance, a method combining multiple shooting, the interval Krawczyk method and the use of the  $C^1$ -Lohner algorithm to integrate the flow was introduced in [5] to obtain rigorous estimates for the monodromy matrix. An important difference is that our method does not rely on a rigorous time integration of the flow. Another important motivation for developing such method is that the computation of invariant bundles of periodic orbits is one of the key ingredient and one of the main difficulty in applying the parameterization method to compute invariant manifold of periodic orbits of a concrete equation (e.g. see [6, 7, 8]). In fact, once the Floquet normal form and the invariant bundles are explicitly known, the computation of higher order terms is rather straightforward. Hence, we believe that developing a general method to compute Floquet normal form is important.

Let us now introduce the ideas behind the rigorous method. The first step is to substitute the Floquet normal form  $\Phi(t) = Q(t)e^{Rt}$  in the differential equation (1). From this, it follows that  $(R, Q(t))$  is a solution of the differential equation with periodic coefficients  $\dot{Q} = A(t)Q - QR$ . On the converse, if a real constant matrix  $R$  and a  $2\tau$ -periodic matrix function  $Q(t)$  solve

$$\begin{cases} \dot{Q} = A(t)Q - QR \\ Q(0) = I, \end{cases} \quad (3)$$

then the matrix function  $\Phi(t) \stackrel{\text{def}}{=} Q(t)e^{Rt}$  is the principal fundamental solution of (1). Therefore, the problem of computing fundamental matrix solutions in the form  $\Phi(t) = Q(t)e^{Rt}$  reduces to find  $(R, Q(t))$  satisfying (3). The next step is to introduce a nonlinear operator  $f$  (see Section 2.1 for details) whose zeros are in one-to-one correspondence with the solutions of (3). Letting  $x = (R, Q_0, Q_1, Q_2, \dots)$ , where the  $Q_k$ 's are the Fourier coefficients of  $Q(t)$ , the problem of computing Floquet normal forms  $\Phi(t) = Q(t)e^{Rt}$  is then equivalent

to find  $x$  such that  $f(x) = 0$ . By the a priori knowledge of the smoothness of  $Q(t)$ , the Fourier coefficients  $Q_k$ 's decay fast, meaning that the solutions of  $f(x) = 0$  live in a suitable Banach space  $\Omega^s$  of rapidly decaying coefficients.

Based on the previous discussion, the next step consists of computing a numerical approximation  $\bar{x}$  of  $f(x) = 0$  and to demonstrate that close to  $\bar{x}$ , there exists a genuine solution  $x^*$  of  $f(x) = 0$ , corresponding to the Floquet normal form of the principal fundamental matrix solution  $\Phi(t)$  of (1). However, since the operator  $f$  is infinite dimensional, a finite dimensional approximation of  $f$  must be introduced in order to compute an approximation  $\bar{x}$ . This is done in Section 2.2. Once  $\bar{x}$  is computed, a Newton-like operator  $T : \Omega^s \rightarrow \Omega^s$  defined by  $T(x) = x - Af(x)$  is introduced, where  $A$  is an injective linear operator which acts as an approximation for  $Df(\bar{x})^{-1}$ . Since  $A$  is injective, the fixed points of  $T$  and the zeros of  $f$  are in one-to-one correspondence. The next step is to consider small balls  $B_{\bar{x}}(r) \subset \Omega^s$  centered at the numerical approximation  $\bar{x}$ , and to solve for  $r$  for which  $T : B_{\bar{x}}(r) \rightarrow B_{\bar{x}}(r)$  is a contraction (see Section 2.3). This verification is done via the use of the notion of the so-called *radii polynomials* (first introduced in [9]) which provide, in the context of differential equations, an efficient means of determining a domain on which the contraction mapping theorem is applicable. The radii polynomials are introduced in Section 2.4, and we present the explicit bounds in Section 2.5 that lead directly to their construction.

The numerical results reported in this paper are only for the case when the state space is three-dimensional and the nonlinearities of the vector fields are quadratic. These restrictions allows on the one hand more complete visualization and on the other hand allows presenting applications in a simple fashion. Increasing the dimension of the systems is straightforward and increasing the degree of the polynomial nonlinearities should also be straightforward, at least theoretically, by applying the analytic estimates of [10]. Let us mention that for the moment, our method does not apply to vector fields with non polynomial nonlinearities since we need explicit control on the Fourier coefficients of the nonlinear terms.

The paper is organized as follows. In Section 2, we introduce the rigorous computational method to compute Floquet normal forms of fundamental matrix solutions. In Section 3, we demonstrate how to use the information from Floquet normal forms to compute stable and unstable bundles of periodic orbits of vector field and how to determine the linear stability properties of periodic orbits using that information. In Section 4, we combine the ideas of Section 2 and Section 3 to construct rigorously stable and unstable bundles of some periodic orbits of the Lorenz equations (Section 4.1) and of the  $\zeta^3$ -model (Section 4.2). Finally, in Section 4.3, we discuss how to recover a posteriori the Floquet multipliers associated to the periodic orbit  $\gamma(t)$ , that is the eigenvalues of the monodromy matrix.

## 2 Rigorous computation of Floquet normal forms

In this section, we introduce the rigorous numerical method to compute Floquet normal forms  $\Phi(t) = Q(t)e^{Rt}$  of fundamental matrix solutions of systems of the form (1). As already mentioned in Section 1, the first step is to introduce a nonlinear operator  $f$  whose zeros are in one-to-one correspondence with the solutions of (3).

### 2.1 Set-up of the operator equation $f(x) = 0$

In the following  $Mat(n, \mathbb{R})$ ,  $Mat(n, \mathbb{C})$  denote the space of  $n \times n$  matrices respectively with real and complex entries. The assumption on  $Q(t)$  to be real and  $2\tau$ -periodic allows to

consider the expansion

$$Q(t) = Q_0 + \sum_{k \in \mathbb{Z} \setminus \{0\}} (Q_{k,1} + iQ_{k,2}) e^{ik\frac{2\pi}{2\tau}t}, \quad (4)$$

where the Fourier coefficients  $Q_0, Q_{k,i} \in Mat(n, \mathbb{R})$  satisfy  $Q_{-k,1} = Q_{k,1}$  and  $Q_{-k,2} = -Q_{k,2}$  for any  $k \geq 1$ . Being  $\tau$ -periodic, the matrix-valued function  $A(t)$  is also  $2\tau$ -periodic, thus it makes sense to consider the expansion

$$A(t) = \sum_{k \in \mathbb{Z}} \mathcal{A}_k e^{ik\frac{2\pi}{2\tau}t}, \quad (5)$$

where  $\mathcal{A}_0 \in Mat(n, \mathbb{R})$ , while the matrices  $\mathcal{A}_k \in Mat(n, \mathbb{C})$  satisfy  $\mathcal{A}_{-k} = \mathcal{C}(\mathcal{A}_k)$ , for any  $k \geq 1$ . Here  $\mathcal{C}(\mathcal{A})$  stands for the matrix whose entries are the complex conjugates of the entries of  $\mathcal{A}$ . It has to be remarked that the assumption for  $A$  to be  $\tau$ -periodic implies that  $\mathcal{A}_k = 0$  for  $k$  odd and  $\mathcal{A}_{2l} = \hat{\mathcal{A}}_l$  where  $\hat{\mathcal{A}}_l$  is the  $l$ -th Fourier coefficient of  $\mathcal{A}(t)$  in the basis  $\{e^{ik\frac{2\pi}{T}t}\}_k$ .

After substituting the expansions (4) and (5) in problem (3), the latter system of ODEs moves into an equation  $F(t) = 0$ , where  $F(t)$  is a  $2\tau$ -periodic matrix function. By a subsequent projection of  $F(t)$  in the Fourier basis  $\{e^{ik\frac{2\pi}{2\tau}t}\}$ , it follows that solving (3) is equivalent to solve for the unknowns

$$R, Q_0 \in Mat(n, \mathbb{R}) \text{ and } Q_k \stackrel{\text{def}}{=} (Q_{k,1}, Q_{k,2}) \in Mat(n, \mathbb{R})^2$$

the infinite dimensional algebraic system

$$\begin{aligned} f(R, Q_0, \dots, Q_k, \dots) &= 0 \\ f &= (f_*, f_0, f_1, \dots, f_k, \dots) \end{aligned} \quad (6)$$

defined by

$$\begin{aligned} f_* &\stackrel{\text{def}}{=} Q_0 + 2 \sum_{k \geq 1} Q_{k,1} - I \\ f_0 &\stackrel{\text{def}}{=} Q_0 R - (A \cdot Q)_0 \\ f_k &\stackrel{\text{def}}{=} \begin{bmatrix} f_{k,1} \\ f_{k,2} \end{bmatrix} = \begin{bmatrix} -k\frac{2\pi}{2\tau}Q_{k,2} + Q_{k,1}R - (A \cdot Q)_{k,1} \\ k\frac{2\pi}{2\tau}Q_{k,1} + Q_{k,2}R - (A \cdot Q)_{k,2} \end{bmatrix}, \quad k \geq 1 \end{aligned} \quad (7)$$

where  $(A \cdot Q)_{k,1}, (A \cdot Q)_{k,2}$  denote respectively the real and imaginary part of the convolution

$$(A \cdot Q)_k \stackrel{\text{def}}{=} \sum_{k_1+k_2=k} \mathcal{A}_{k_1} (Q_{k_2,1} + iQ_{k_2,2}).$$

Note that  $f_*, f_0 \in Mat(n, \mathbb{R})$  and  $f_k \in Mat(n, \mathbb{R})^2$  for every  $k \geq 1$ .

The problem (6) consists of: *i*) a system of  $n^2$  real scalar equations for  $f_* = 0$  representing the initial condition  $Q(0) = I$ ; *ii*)  $n^2$  real scalar equations for system  $f_0 = 0$  that reproduces  $\langle F(t), 1 \rangle = 0$ ; *iii*)  $2n^2$  real scalar equations for each  $f_k = 0$  ( $k \geq 1$ ). Note that  $f_{k,1}, f_{k,2}$  are the real and complex part of the equation  $\langle F(t), e^{ik\frac{2\pi}{2\tau}t} \rangle = ik\frac{2\pi}{2\tau}Q_k + Q_kR - (\mathcal{A} \cdot Q)_k$ . Here,  $\langle \cdot, \cdot \rangle$  represents the inner product in  $L^2([0, \frac{2\pi}{2\tau}])$ .

Before proceeding with the analysis of the system  $f = 0$  given by (6), let us introduce some notation that will be adopted throughout the paper.

*Notation*

Let  $A, B$  be matrices with entries  $A = \{a_{i,j}\}$ ,  $B = \{b_{i,j}\}$  and  $\mathcal{A} = (A_1, \dots, A_n)$ ,  $\mathcal{B} = (B_1, \dots, B_n)$  be vectors of matrices. Denote by

- i)  $|A| = \{|a_{i,j}|\}$  the matrix of absolute values, where  $|\cdot|$  denotes both the real and complex absolute value, according with  $a_{i,j}$ . For vectors  $|\mathcal{A}| = (|A_1|, \dots, |A_n|)$ ;  $|A|_\infty = \max_{i,j} \{|a_{i,j}|\}$  and  $|\mathcal{A}|_\infty = \max\{|A_1|_\infty, \dots, |A_n|_\infty\}$
- ii)  $A \leq_{cw} B$  means  $a_{i,j} \leq b_{i,j}$  for any  $i, j$ . In case  $b$  is a scalar,  $A \leq_{cw} b$  means  $a_{i,j} \leq b$ . In case of vectors  $\mathcal{A} \leq_{cw} \mathcal{B}$  and  $\mathcal{A} \leq_{cw} b$  extends as  $A_k \leq_{cw} B_k$  and  $A_k \leq_{cw} b$ , for any  $k = 1 \dots n$ . The same for  $\geq_{cw}, >_{cw}, <_{cw}$ ;
- iii)  $\|A\|_\infty$  is the standard infinity norm of a matrix:  $\|A\|_\infty = \max_i \sum_j |a_{i,j}|$ ;
- iv)  $I$  denotes the identity  $n \times n$  matrix,  $\mathbb{1}_n$  is the  $n \times n$  matrix whose entries are all 1.

Coming back to the analysis of system (6) let us define the space

$$X = \left\{ x = (x_0, x_1, \dots, x_k, \dots) : \begin{array}{l} x_0 = (R, Q_0) \in \text{Mat}(n, \mathbb{R})^2 \\ x_k = Q_k = (Q_{k,1}, Q_{k,2}) \in \text{Mat}(n, \mathbb{R})^2, k \geq 1 \end{array} \right\}.$$

Note that  $f : X \rightarrow X$ . Later on the problem of solving  $f = 0$  will be transformed into a fixed point problem for an operator  $T$ : that requires the choice of a suitable Banach subspace of  $X$  where to investigate the existence of solutions. To define the proper Banach space, let us first introduce the weigh function

$$w_k = \begin{cases} |k| & k \neq 0 \\ 1 & k = 0 \end{cases} \quad (8)$$

and given  $x = (R, Q_0, Q_{1,1}, Q_{1,2}, \dots, Q_{k,1}, Q_{k,2}, \dots) \in X$ , let us define the  $s$ -norm of  $x$  in  $X$  by

$$\|x\|_s \stackrel{\text{def}}{=} \sup_{k \geq 0} \{|x_k|_\infty w_k^s\} = \sup \left\{ |R|_\infty, |Q_0|_\infty, \sup_{k \geq 1} \{|Q_{k,1}|_\infty w_k^s, |Q_{k,2}|_\infty w_k^s\} \right\}.$$

According with the  $s$ -norm, let us define the space  $\Omega^s$  of sequences in  $X$  with algebraically decaying tails

$$\Omega^s = \{x \in X : \|x\|_s < \infty\}. \quad (9)$$

For any  $s > 0$  the space  $\Omega^s$  endowed with the  $s$ -norm is a Banach space and the inclusion  $\Omega^s \supset \Omega^{s+1}$  holds. The introduction of  $\Omega^s$  is motivated by the fact that a periodic solution  $Q(t)$  of system (3) results to be at least as smooth as  $A(t)$ . Thus, in case the function  $A(t)$  is analytic, it follows that  $Q(t)$  is analytic. As a consequence the Fourier coefficients of  $Q(t)$  decay faster than any power rate and therefore they live in  $\Omega^s$  for any  $s$ . On the other hand, even a weaker assumption of the function  $A(t)$ , such as a  $|\mathcal{A}_k|_\infty < Cw_k^{-s}$  for a constant  $C$  and positive  $s$ , allows to conclude that the solution  $x \in \Omega^s$ . The latter is the case we are mainly interested in. Indeed, for the sake of generality and to emphasize the robustness and versatility of the technique, one assumes the weakest assumption on  $\mathcal{A}_k$  that makes the computational method applicable. Such assumption is that there exists  $s \geq 2$  and a constant  $C > 0$  such that the coefficient  $\mathcal{A}_k$  satisfy  $|\mathcal{A}_k|_\infty < Cw_k^{-s}$ . This condition implies that an integrable function  $A(t)$  with expansion as in (5) is differentiable up to order  $s - 1$ .

Denote with  $\mathcal{A} = \{\mathcal{A}_k\}_{k \geq 0}$  the sequence of the Fourier coefficients appearing in (5) and, as an extension of the  $s$ -norm, define

$$\|\mathcal{A}\|_s = \sup_{k \geq 0} \{|\mathcal{A}_k|_\infty w_k^s\}. \quad (10)$$

**Lemma 2.1.** *Assume  $\|\mathcal{A}\|_{s^*} < \infty$  for  $s^* \geq 2$ . Then  $f$  maps  $\Omega^s$  in  $\Omega^{s-1}$ , for any  $2 \leq s \leq s^*$ .*

*Proof.* Let  $2 \leq s \leq s^*$  and suppose  $x \in \Omega^s$ . Then  $|\mathcal{A}_k|_\infty < C_1 w_k^{-s}$  and, from Lemma 2.1 in [10],  $|(\mathcal{A} \cdot Q)_k|_\infty \leq \frac{C_2}{w_k^s}$ . Thus  $|f_k(x)|_\infty \leq C_3 k |Q_k|_\infty + C_4 |Q_k|_\infty + C_2 w_k^{-s} < C w_k^{-s+1}$ , for suitable constants  $C, C_i$ . This shows that  $f(x) \in \Omega^{s-1}$ .  $\blacksquare$

Thus we will look for solutions of the system (6) within the space  $\Omega^s$  for some  $s \geq 2$ . The idea is to reformulate the zero finding problem  $f(x) = 0$  as a fixed point problem for a suitable operator  $T$  defined in  $\Omega^s$  and to verify the hypothesis of the contraction mapping theorem in order to conclude about the existence of a fixed point. More explicitly, the idea is to prove the existence of a ball  $B_{\bar{x}}(r)$  in  $\Omega^s$  around a finite dimensional approximate solution  $\bar{x}$  on which the operator  $T$  is a contraction. The proof will follow by verifying a finite number of polynomial inequalities: the so-called *radii polynomials*. Their computation will result from rigorous numerical computations and analytic estimates. The next step is to compute a finite dimensional approximate solution  $\bar{x}$ . For this, one needs to introduce a finite dimensional projection of  $f(x) = 0$  given by (6).

## 2.2 Finite dimensional projection

As mentioned earlier, the first step involved in the computational method is to consider a finite dimensional projection and to compute an approximate numerical solution of (6).

For  $m > 1$  consider the finite dimensional space  $X^m = \prod_{k=1}^m \text{Mat}(n, \mathbb{R})^2$  and define the projections

$$\begin{aligned} \Pi_m : X &\rightarrow X^m \\ x &\mapsto \Pi_m(x) = x^m = (R, Q_0, \dots, Q_{m-1}) \end{aligned}$$

$$\Pi_\infty : x \mapsto (Q_m, Q_{m+1}, \dots)$$

so that  $x = (x^m, \Pi_\infty(x))$ . Denote with  $0^\infty \stackrel{\text{def}}{=} \Pi_\infty(0)$ . Moreover let us define the restricted map

$$\begin{aligned} f^{(m)} : X^m &\rightarrow X^m \\ x^m &\mapsto \Pi_m f(x^m, 0^\infty) \end{aligned} \quad (11)$$

Note that for any  $x \in X$  the sequence  $(x^m, 0^\infty) \in X$  and the finite dimensional projection  $\Pi_m$  applied to  $f(x)$  reads as  $\Pi_m f(x) = (f_*, f_0, \dots, f_{m-1})(x)$ . Since  $X^m$  is isomorphic to  $\mathbb{R}^{m^2 n^2}$ , one can think of  $f^{(m)} : \mathbb{R}^{m^2 n^2} \rightarrow \mathbb{R}^{m^2 n^2}$ . Suppose that using a Newton-like iterative algorithm, one computed

$$\bar{x} = (\bar{R}, \bar{Q}_0, \dots, \bar{Q}_{m-1})$$

an approximate zero of  $f^{(m)}$ , that is  $f^{(m)}(\bar{x}) \approx 0$ . For simplicity the same notation  $\bar{x}$  is used to identify the above vector in  $X^m$  and the sequence  $(\bar{x}, 0^\infty)$  in  $X$ . As already mentioned at the end of Section 2.1, the idea is to consider a ball  $B_{\bar{x}}(r) \in \Omega^s$  centered at the approximate solution  $\bar{x}$  and to show the existence of a contraction mapping  $T$  acting on  $B_{\bar{x}}(r)$ . Hence, let us now introduce the fixed point operator  $T$ .

### 2.3 The fixed point operator $T(x) = x$

In this section, we first define an operator  $T$  on  $\Omega^s$  whose fixed points correspond to solutions of  $f(x) = 0$  and then, we introduce some computable conditions from which one can conclude about the existence of fixed point of  $T$ . To begin with, suppose to have chosen a representation of the matrices  $Mat(n, \mathbb{R})$  as vector in  $\mathbb{R}^{n^2}$  and to have extended it to an isomorphism between the space of sequences of  $N$  matrices  $Mat(n, \mathbb{R})$  to  $\mathbb{R}^{Nn^2}$ . Note that  $X^m$  is isomorphic to  $\mathbb{R}^{m2n^2}$ .

In the sequel, consider a vector  $V = [v_1, \dots, v_{N2n^2}] \in \mathbb{R}^{N2n^2}$ . We denote by  $V_k \in \mathbb{R}^{2n^2}$ ,  $k = 0, \dots, N-1$  the vector with  $2n^2$  components  $V_k = [v_{k2n^2+1}, v_{k2n^2+2}, \dots, v_{(k+1)2n^2}]$ . The reason of this choice of notation is the following: suppose that  $V$  is the vector representation of the sequence  $x = (R, Q_0, Q_1, \dots, Q_{N-1}) \in X^N$  for a positive  $N$ , then  $V_k$  represents the couple  $(R, Q_0)$  when  $k = 0$  and  $Q_k = (Q_{k,1}, Q_{k,2})$  for  $k \geq 1$ .

Denote by  $Df^{(m)}(\bar{x})$  the Jacobian of  $f^{(m)}$  with respect to  $x^m$  evaluated at  $\bar{x}$ , that is

$$Df^{(m)} \stackrel{\text{def}}{=} Df^{(m)}(\bar{x}) = \frac{\partial(f_*, f_0, f_1, \dots, f_{m-1})}{\partial(R, Q_0, \dots, Q_{m-1})}(\bar{x}) \in Mat(2n^2m, \mathbb{R}).$$

For clarity and completeness,

$$Df^{(m)} = \left[ \begin{array}{cccccc} \frac{\partial f_*}{\partial R} & \frac{\partial f_*}{\partial Q_0} & \frac{\partial f_*}{\partial Q_{1,1}} & \frac{\partial f_*}{\partial Q_{1,2}} & \cdots & \frac{\partial f_*}{\partial Q_{m-1,1}} & \frac{\partial f_*}{\partial Q_{m-1,2}} \\ \frac{\partial f_0}{\partial R} & \frac{\partial f_0}{\partial Q_0} & \frac{\partial f_0}{\partial Q_{1,1}} & \frac{\partial f_0}{\partial Q_{1,2}} & & \frac{\partial f_0}{\partial Q_{m-1,1}} & \frac{\partial f_0}{\partial Q_{m-1,2}} \\ \frac{\partial f_1}{\partial(R, Q_0)} & & \frac{\partial f_1}{\partial Q_1} & & \cdots & & \frac{\partial f_1}{\partial Q_{m-1}} \\ \vdots & & \vdots & & \vdots & & \vdots \\ \frac{\partial f_{m-1}}{\partial(R, Q_0)} & & \frac{\partial f_{m-1}}{\partial Q_1} & & \cdots & & \frac{\partial f_{m-1}}{\partial Q_{m-1}} \end{array} \right](\bar{x}) \quad (12)$$

where for  $k, j = 1, \dots, m-1$

$$\frac{\partial f_k}{\partial(R, Q_0)} = \left[ \begin{array}{cc} \frac{\partial f_{k,1}}{\partial R} & \frac{\partial f_{k,1}}{\partial Q_0} \\ \frac{\partial f_{k,2}}{\partial R} & \frac{\partial f_{k,2}}{\partial Q_0} \end{array} \right], \quad \frac{\partial f_k}{\partial Q_j} = \left[ \begin{array}{cc} \frac{\partial f_{k,1}}{\partial Q_{j,1}} & \frac{\partial f_{k,1}}{\partial Q_{j,2}} \\ \frac{\partial f_{k,2}}{\partial Q_{j,1}} & \frac{\partial f_{k,2}}{\partial Q_{j,2}} \end{array} \right],$$

and each  $\frac{\partial f_{k,i}}{\partial Q_{j,l}} \in Mat(n^2, \mathbb{R})$  denotes the Jacobian matrix of the components of  $f_{k,j}$  with respect to the components of  $Q_{j,l}$ .

Moreover, for  $k \geq m$ , let be defined

$$\Lambda_k \stackrel{\text{def}}{=} \frac{\partial f_k}{\partial Q_k}(\bar{x}) \in Mat(2n^2, \mathbb{R}).$$

**Lemma 2.2.** Recall (5) and (10), and assume that  $\|\mathcal{A}\|_s < \infty$  for some  $s \geq 2$ . Then there exist two constants  $K$  and  $C_\Lambda$  such that for any  $k \geq K$  the linear operator  $\Lambda_k$  is invertible and  $\|\Lambda_k^{-1}\|_\infty < \frac{C_\Lambda}{k}$ . The constants  $K$  and  $C_\Lambda$  depend on  $\|\mathcal{A}\|_s$ , the period  $\tau$  and  $|\bar{R}|_\infty$ .

*Proof.* The real and imaginary parts of  $(A \cdot Q)_k$  can be written explicitly as

$$(A \cdot Q)_{k,1} = (Re(\mathcal{A}_0) + Re(\mathcal{A}_{2k}))Q_{k,1} + Im(\mathcal{A}_{2k})Q_{k,2} + W_1$$

$$(A \cdot Q)_{k,2} = Im(\mathcal{A}_{2k})Q_{k,1} + (Re(\mathcal{A}_0) - Re(\mathcal{A}_{2k}))Q_{k,2} + W_2$$

where  $W_1$  and  $W_2$  do not depend on  $Q_{k,1}$  and  $Q_{k,2}$ . Thus, looking at the definition of  $f_k$  in (7), it follows that  $\Lambda_k$  is of the form

$$\Lambda_k = \begin{bmatrix} \lambda_{1,1} & -k \frac{2\pi}{2\tau} \mathbb{I}_{n^2} + \lambda_{1,2} \\ k \frac{2\pi}{2\tau} \mathbb{I}_{n^2} + \lambda_{2,1} & \lambda_{2,2} \end{bmatrix}, \quad (13)$$

where the entries of  $\lambda_{1,1}$  and  $\lambda_{2,2}$  are linear combination of the entries of  $\bar{R}$ ,  $\mathcal{A}_0$ ,  $\mathcal{A}_{2k}$  so that  $|\lambda_{1,1}|_\infty, |\lambda_{2,2}|_\infty < |\bar{R}|_\infty + |\mathcal{A}_0|_\infty + |\mathcal{A}_{2k}|_\infty$  holds. Also,  $\lambda_{2,1} = \lambda_{1,2}$  only depend on  $\mathcal{A}_{2k}$ . By a row permutation, the invertibility of  $\Lambda_k$  is equivalent to the invertibility of

$$\hat{\Lambda}_k = \begin{bmatrix} k \frac{2\pi}{2\tau} \mathbb{I}_{n^2} + \lambda_{2,1} & \lambda_{2,2} \\ \lambda_{1,1} & -k \frac{2\pi}{2\tau} \mathbb{I}_{n^2} + \lambda_{1,2} \end{bmatrix}.$$

Since  $|\lambda_{1,1}|_\infty, |\lambda_{2,2}|_\infty < |\bar{R}|_\infty + |\mathcal{A}_0|_\infty + |\mathcal{A}_{2k}|_\infty$  and  $|\lambda_{1,2}|_\infty < |\mathcal{A}_{2k}|_\infty$ , the assumption  $\|\mathcal{A}\|_s < \infty$  implies that the  $|\lambda_{i,j}|_\infty$  are uniformly bounded in  $k$ , and moreover  $|\lambda_{1,2}|_\infty$  is decreasing. Thus there exists  $K$  such that  $\hat{\Lambda}_k$  is diagonally dominant for any  $k \geq K$ . This is enough to conclude that  $\hat{\Lambda}_k$  is invertible for any  $k \geq K$ .

Denote by  $a_{i,i}$  the diagonal elements of  $\hat{\Lambda}_k$ . Hence, if  $\hat{\Lambda}_k$  is diagonally dominant, that is if  $|a_{i,i}| > \sum_{j \neq i} |\hat{\Lambda}_k(i,j)|$  for any  $i = 1, \dots, 2n^2$ , then using a result from [11], one gets the following bound

$$\|\hat{\Lambda}_k^{-1}\|_\infty \leq \max_i \left\{ \frac{1}{|a_{i,i}| - \sum_{j \neq i} |\hat{\Lambda}_k(i,j)|} \right\}.$$

Therefore, for  $k \geq K$

$$\|\Lambda_k^{-1}\|_\infty = \|\hat{\Lambda}_k^{-1}\|_\infty \leq \frac{C_\Lambda}{k}$$

for a constant  $C_\Lambda$  depending on  $\tau$ ,  $\bar{R}$ ,  $|\mathcal{A}_0|_\infty$  and  $|\mathcal{A}_{2k}|_\infty$ . ■

Given  $M > m$ , let be defined the operator  $L_M : X^M \rightarrow X^M$  represented by

$$L_M = \left[ \begin{array}{c|ccc} & \frac{\partial f_*}{\partial Q_m}(\bar{x}) & \dots & \frac{\partial f_*}{\partial Q_{M-1}}(\bar{x}) \\ \hline Df^{(m)} & 0 & \dots & 0 \\ & 0 & \dots & 0 \\ & & & \ddots \\ & & & \Lambda_{M-1} \end{array} \right] \quad (14)$$

Suppose to have numerically computed an invertible matrix  $A_m \in Mat(2n^2m, \mathbb{R})$  as approximation of  $(Df^{(m)})^{-1}$

$$A_m \cdot Df^{(m)} \approx I$$

and use such matrix to construct an invertible linear operator  $A_M : X^M \rightarrow X^M$

$$A_M \stackrel{\text{def}}{=} \left[ \begin{array}{c|c} A_m & \mathcal{L} \\ \hline & (\Lambda_m)^{-1} \\ & \ddots \\ & (\Lambda_{M-1})^{-1} \end{array} \right], \quad \text{such that } A_M \cdot L_M \approx I \quad (15)$$

By straightforward calculations, the matrix  $\mathcal{L}$  can be easily constructed combining the matrix  $A_m$  with the matrices  $\{(\Lambda_k)^{-1}, \frac{\partial f_*}{\partial Q_k}(\bar{x})\}_{k=m}^{M-1}$ . More explicitly, writing

$$\mathcal{L} = \left[ \begin{array}{c|c|c|c} \mathcal{L}_m & \mathcal{L}_{m+1} & \dots & \mathcal{L}_{M-1} \end{array} \right], \quad \mathcal{L}_k \in Mat([2n^2m, 2n^2]; \mathbb{R})$$

we can construct  $\mathcal{L}$  by  $\mathcal{L}_k = -2(A_m)^{[1 \dots n^2]} \cdot (\Lambda_m^{-1})_{[1, \dots, n^2]}$ , where  $A^{[1, \dots, k]}$ ,  $(A_{[1, \dots, k]})$  denotes the submatrix of  $A$  given by the first  $k$  columns (rows) of  $A$ .

The idea behind the definition of  $L_M$  is to collect the differential of  $f^{(m)}$  at the point  $\bar{x}$  and the linear terms of the larger projection  $f^{(M)}$  so that the operator  $A_M$  is not so far from being a good approximation of the inverse of  $Df^{(M)}(\bar{x})$ , and not only of  $Df^{(m)}$ .

We are now ready to introduce the fixed point operator. For a choice of the finite dimensional parameter  $m > K$  where  $K$ , as defined in Lemma 2.2, is such that  $\Lambda_k$  is invertible for any  $k \geq K$ , and a choice of the computational parameter  $M > m$ , a formal diagonal concatenation of the operator  $A_M$  and the sequence  $\Lambda_k^{-1}$ , for  $k \geq M$ , produces the linear operator

$$\begin{aligned} A : X &\rightarrow X \\ x &\mapsto Ax \\ (Ax)_k &\stackrel{\text{def}}{=} \begin{cases} (A_M x^M)_k & k = 0, \dots, M-1 \\ \Lambda_k^{-1} Q_k & k \geq M. \end{cases} \end{aligned} \tag{16}$$

We define the operator  $T$  on  $X$  as

$$T(x) \stackrel{\text{def}}{=} x - Af(x),$$

and denote  $T_k(x) = (T(x))_k$ .

**Lemma 2.3.** *Recall (5) and (10), and assume that  $\|\mathcal{A}\|_{s^*} < \infty$  for  $s^* \geq 2$ . Then for any  $2 \leq s \leq s^*$ ,  $T : \Omega^s \rightarrow \Omega^s$  and solutions of  $T(x) = x$  correspond to solutions of  $f(x) = 0$ .*

*Proof.* From Lemma 2.1, given  $x \in \Omega^s$  it follows that  $f(x) \in \Omega^{s-1}$ . The linear operator  $A$  maps  $\Omega^{s-1}$  in  $\Omega^s$ . Indeed for  $k \geq M$ ,  $|(Ax)_k|_\infty = |\Lambda_k^{-1} x_k|_\infty \leq \|\Lambda_k^{-1}\|_\infty |x_k|_\infty$ . Thus from Lemma 2.2 and assuming  $x \in \Omega^{s-1}$ , it follows that  $|(Ax)_k|_\infty \leq \frac{C}{k} \frac{\|x\|_{s-1}}{w_k^{s-1}} < \frac{C_1}{w_k^s}$ , for positive constants  $C, C_1$ . This proves that  $T : \Omega^s \rightarrow \Omega^s$ . Since  $A_M$  is invertible by assumption and  $\Lambda_k$  have been proved in Lemma 2.2 to be invertible for all  $k \geq m > K$ , it follows that the linear operator  $A$  is invertible and therefore fixed points of  $T$  correspond to zeros of  $f(x)$ . ■

By construction, when restricted to the finite dimensional projection  $\Pi_m \Omega^s$ , the operator  $T$  acts as  $T(x^m) = x^m - A_m f^{(m)}(x^m)$ . Thus on  $\Pi_m \Omega^s$ ,  $T$  is close to the Newton operator: the only difference is that point where the derivative is computed does not change along the iteration process. Therefore we can consider  $T$  as an extension to a infinite dimensional space of a finite dimensional Newton-like operator.

The existence of a fixed point for the operator  $T$  will be assured by the Banach Fixed Point Theorem once the operator  $T$  has been proved to be a contraction on a suitable ball in  $\Omega^s$ . The suitable ball on which  $T$  will be proved to be a contraction will be sought within the family of balls  $B_{\bar{x}}(r) \in \Omega^s$

$$B_{\bar{x}}(r) = \bar{x} + B(r)$$

where  $B(r)$  is the ball of radius  $r$  in  $\Omega^s$  centered in the origin and  $r$  is treated as variable. Following the same approach as in different other papers, we are going to construct a finite set of computable conditions, the so-called *radii polynomials* (first introduced in [9]), to be solved in  $r$ , whose verification implies that the hypothesis of the Banach Fixed Point Theorem are satisfied. In practice, the radii polynomials are defined as realization of the hypotheses of the following theorem.

Suppose there exist two matrices sequences

$$Y = (Y_0, Y_1, \dots, Y_k, \dots), \quad Z(r) = (Z_0, Z_1, \dots, Z_k, \dots)(r), \quad Y, Z \in X$$

such that

$$|(T(\bar{x}) - \bar{x})_k| \leq_{cw} Y_k, \quad \sup_{b_1, b_2 \in B(r)} \left| [DT(\bar{x} + b_1)b_2]_k \right| \leq_{cw} Z_k(r), \quad \forall k \geq 0. \quad (17)$$

**Theorem 2.4.** Fix  $s \geq 2$  and let  $Y$  and  $Z$  defined as in (17). If there exists  $r > 0$  such that  $\|Y + Z\|_s < r$ , then the operator  $T$  maps  $B_{\bar{x}}(r)$  into itself and  $T : B_{\bar{x}}(r) \rightarrow B_{\bar{x}}(r)$  is a contraction. Thus, by the Banach Fixed Point Theorem, there exists an unique  $x^* \in B_{\bar{x}}(r)$  solution of  $T(x^*) = x^*$  and therefore solution of  $f(x^*) = 0$ .

*Proof.* Two statements need to be proved:

- i)  $T(B_{\bar{x}}(r)) \subset B_{\bar{x}}(r)$ , that is  $\|T(x) - \bar{x}\|_s < r$  for all  $x \in B_{\bar{x}}(r)$ ,
- ii)  $T$  is a contraction, that is there exists  $\kappa \in (0, 1)$  such that for every  $x, y \in B_{\bar{x}}(r)$ , one has that  $\|T(x) - T(y)\|_s \leq \kappa \|x - y\|_s$ .

For a given  $k \geq 0$  and any  $x, y \in B_{\bar{x}}(r)$ , the mean value theorem implies

$$T_k(x) - T_k(y) = DT_k(z)(x - y)$$

for some  $z \in \{tx + (1-t)y : t \in [0, 1]\} \subset B_{\bar{x}}(r)$ . Note that  $r \frac{(x-y)}{\|x-y\|_s} \in B(r)$  thus for (17)

$$|T_k(x) - T_k(y)| = \left| DT_k(z) \frac{r(x-y)}{\|x-y\|_s} \right| \frac{1}{r} \|x - y\|_s \leq_{cw} \frac{Z_k(r)}{r} \|x - y\|_s \quad (18)$$

The triangular inequality applied component-wise gives

$$|T_k(x) - \bar{x}_k| \leq_{cw} |T_k(x) - T_k(\bar{x})| + |T_k(\bar{x}) - \bar{x}_k| \leq_{cw} Y_k + Z_k(r)$$

hence

$$|T_k(x) - \bar{x}_k|_\infty \leq |Y_k + Z_k(r)|_\infty.$$

Therefore for any  $x \in B_{\bar{x}}(r)$

$$\|T(x) - \bar{x}\|_s = \sup_{k \geq 0} \{|T_k(x) - \bar{x}_k|_\infty w_k^s\} \leq \sup_{k \geq 0} \{|Y_k + Z_k(r)|_\infty w_k^s\} = \|Y + Z(r)\|_s < r.$$

This proves i).

Again from (18), for any  $x, y \in B_{\bar{x}}(r)$ ,  $|T_k(x) - T_k(y)|_\infty \leq \frac{|Z_k(r)|_\infty}{r} \|x - y\|_s$ , thus

$$\|T(x) - T(y)\|_s \leq \frac{\|Z(r)\|_s}{r} \|x - y\|_s \quad (19)$$

Note that all the entries of  $Y_k$  and  $Z_k(r)$  are non negative, thus  $|Z_k(r)|_\infty \leq |Y_k + Z_k(r)|_\infty$  and  $\|Z(r)\|_s \leq \|Y + Z(r)\|_s < r$ . That implies that

$$\kappa \stackrel{\text{def}}{=} \frac{\|Z(r)\|_s}{r} \in (0, 1),$$

and we can conclude the proof of ii). An application of the Banach Fixed Point Theorem on the Banach space  $B_{\bar{x}}(r)$  gives the existence and unicity of a solution  $x^*$  of the equation  $T(x) = x$  in  $B_{\bar{x}}(r)$  and, from Lemma 2.3, of a solution of  $f(x) = 0$ .  $\blacksquare$

## 2.4 The radii polynomials

As already mentioned in Section 1, the radii polynomials are a set of  $r$ -dependent polynomials  $p_k(r)$  defined in such a way that if  $r^*$  is a common solution of  $p_k(r^*) < 0$ , then the ball  $B_{\bar{x}}(r^*) \subset \Omega^s$  of radius  $r^*$  centered at the numerical approximation  $\bar{x}$  contains a unique solution of  $f(x) = 0$ . This is due to the fact that by construction of the polynomials, one has that  $\|Y + Z(r^*)\|_s < r^*$ , meaning that the hypotheses of Theorem 2.4 are satisfied. In terms of the components, the formula  $\|Y + Z(r)\|_s < r$  reads as

$$|Y_k + Z_k(r)|_\infty - \frac{r}{w_k^s} < 0, \quad \forall k \geq 0. \quad (20)$$

The latter consists of a system of infinitely many inequalities, which is then impossible to be verify directly with computations. In order to reduce (20) to a finite number of inequalities, suppose that, for a given  $M$ , there exist  $Y_M$  and  $Z_M(r)$  such that

$$|(T(\bar{x}) - \bar{x})_k|_\infty \leq \frac{M^s}{k^s} Y_M, \quad \sup_{b_1, b_2 \in B(r)} \left| [DT(\bar{x} + b_1)b_2]_k \right|_\infty \leq \frac{M^s}{k^s} Z_M(r), \quad \forall k \geq M, \quad (21)$$

and introduce the set of  $M + 1$  radii polynomials as follows.

**Definition 2.5.** The *radii polynomials* are defined as

$$\begin{aligned} p_k(r) &\stackrel{\text{def}}{=} Y_k + Z_k(r) - \frac{r}{w_k^s} (\mathbb{1}_n, \mathbb{1}_n), \quad k = 0, \dots, M-1 \\ p_M &\stackrel{\text{def}}{=} Y_M + Z_M(r) - \frac{r}{w_M^s}. \end{aligned} \quad (22)$$

**Theorem 2.6.** Consider  $M$  and let  $Y, Z$  such that  $Y_k, Z_k$  satisfy (17) for  $k = 0, \dots, M-1$  while for  $k \geq M$  define

$$Y_k \stackrel{\text{def}}{=} \frac{M^s}{k^s} Y_M [\mathbb{1}_n, \mathbb{1}_n], \quad Z_k(r) \stackrel{\text{def}}{=} \frac{M^s}{k^s} Z_M [\mathbb{1}_n, \mathbb{1}_n],$$

where  $Y_M, Z_M$  satisfy the tail condition (21). If there exists  $r > 0$  such that  $p_k(r) <_{cw} 0$  for all  $k = 0, \dots, M$ , then there exists a unique  $x^* \in B_{\bar{x}}(r)$  such that  $T(x^*) = x^*$  and  $f(x^*) = 0$ .

*Proof.* Since by definition  $Y_k \geq_{cw} 0, Z_k \geq_{cw} 0$ , the relations  $p_k(r) <_{cw} 0$  imply that  $|Y_k + Z_k(r)|_\infty < \frac{r}{w_k^s}$  for  $k = 0, \dots, M-1$ . For  $k \geq M$ ,  $Y_k, Z_k$  satisfy (17) and from  $Y_M + Z_M(r) - \frac{r}{w_M^s} < 0$ , it follows that  $|Y_k + Z_k(r)|_\infty - \frac{r}{w_k^s} < 0$ . Indeed

$$|Y_k + Z_k(r)|_\infty = \frac{M^s}{k^s} (Y_M + Z_M) < \frac{M^s}{k^s} \frac{r}{M^s}, \quad \forall k \geq M.$$

Hence

$$\|Y + Z\|_s = \sup_{k \geq 0} \{|Y_k + Z_k| w_k^s\} < r,$$

and the result follows from Theorem 2.4. ■

## 2.5 Construction of the bounds $Y, Z$

This section is devoted to the construction of the matrices  $Y_k, Z_k$  satisfying (17), and of the asymptotic bounds  $Y_M, Z_M$  satisfying (21). This construction provides the complete description of the radii polynomials introduced in Definition 2.5. With the aim of remaining as general as possible, the only constraint we assume on the  $\tau$ -periodic function  $A(t)$  is that

the vector of Fourier coefficients  $\mathcal{A}$  given in (5) satisfies  $\|\mathcal{A}\|_{s^*} < \infty$  for  $s^* \geq 2$ . Nevertheless, further information on the coefficients  $\mathcal{A}_k$  may be useful to get sharper analytical estimates, as it will be manifest in the examples.

In what follows, the growth rate parameter  $s$  has been fixed so that  $2 \leq s \leq s^*$ , the finite dimensional parameter  $m$  has been chosen greater than  $K$ , where  $K$  is a lower bound given by Lemma 2.2 and the computational parameter  $M$  has been chosen so that  $M > m$ . Moreover, assume that one computed  $\Lambda_k^{-1}$  for  $k = m, \dots, M-1$ . Note that in some cases, it will be possible to achieve this task analytically, but in other cases, only an interval enclosure using rigorous numerics will be possible. Also, recalling Lemma 2.2, denote by  $C_\Lambda$  a computable constant such that

$$\|\Lambda_k^{-1}\|_\infty \leq \frac{C_\Lambda}{k}, \text{ for } k \geq m. \quad (23)$$

### 2.5.1 The bound $Y$

By definition,  $T(\bar{x}) - \bar{x} = -Af(\bar{x})$ , thus define  $Y$  as

$$Y_k = \left| \left( A_M f^{(M)}(\bar{x}) \right)_k \right|, \quad k = 0, \dots, M-1 \quad (24)$$

Reminding (21), the tail bound  $Y_M$  has to be defined so that  $Y_M \frac{M^s}{k^s} > |\Lambda_k^{-1} f_k(\bar{x})|_\infty$ , for any  $k \geq M$ . We now introduce a coarse bound  $Y_M$  based on the relation  $|\Lambda_k^{-1} f_k(\bar{x})|_\infty \leq \|\Lambda_k^{-1}\|_\infty |f_k(\bar{x})|_\infty$ . Since  $\bar{Q}_{k,1} = \bar{Q}_{k,2} = 0$  for any  $k \geq m$ , it follows that

$$f_k(\bar{x}) = \begin{bmatrix} -(A \cdot Q)_{k,1} \\ -(A \cdot Q)_{k,2} \end{bmatrix} = \sum_{\substack{k_1+k_2=k \\ |k_2| < m}} \begin{bmatrix} -\operatorname{Re}(\mathcal{A}_{k_1}(\bar{Q}_{k_2,1} + i\bar{Q}_{k_2,2})) \\ -\operatorname{Im}(\mathcal{A}_{k_1}(\bar{Q}_{k_2,1} + i\bar{Q}_{k_2,2})) \end{bmatrix}, \quad \forall k \geq M. \quad (25)$$

Now, using the fact that  $|\mathcal{A}_k|_\infty \leq \|\mathcal{A}\|_{s^*} w_k^{-s^*}$ , both  $|f_{k,1}(\bar{x})|$  and  $|f_{k,2}(\bar{x})|$  are component-wise bounded by

$$\begin{aligned} \left| \sum_{\substack{k_1+k_2=k \\ |k_2| < m}} \mathcal{A}_{k_1}(\bar{Q}_{k_2,1} + i\bar{Q}_{k_2,2}) \right| &\leq_{cw} \sum_{\substack{k_1+k_2=k \\ |k_2| < m}} |\mathcal{A}_{k_1}| |\bar{Q}_{k_2,1} + i\bar{Q}_{k_2,2}| \\ &\leq_{cw} |\mathcal{A}_k| |\bar{Q}_0| + \sum_{l=1}^{m-1} (|\mathcal{A}_{k-l}| + |\mathcal{A}_{k+l}|) |\bar{Q}_{l,1} + i\bar{Q}_{l,2}| \\ &\leq_{cw} \frac{\|\mathcal{A}\|_{s^*}}{w_k^s} \left[ \frac{w_k^s}{w_k^{s^*}} \mathbb{1}_n |\bar{Q}_0| + \sum_{l=1}^{m-1} w_k^s \left( \frac{1}{w_{k+l}^{s^*}} + \frac{1}{w_{k-l}^{s^*}} \right) \mathbb{1}_n |\bar{Q}_{l,1} + i\bar{Q}_{l,2}| \right]. \end{aligned}$$

For  $k \geq M$  the bounds  $\frac{w_k^s}{w_k^{s^*}} \leq 1$  and  $w_k^s \left( \frac{1}{w_{k+l}^{s^*}} + \frac{1}{w_{k-l}^{s^*}} \right) \leq 1 + (1 - \frac{l}{M})^{-s}$  hold, thus one computes the matrix

$$W = \mathbb{1}_n |\bar{Q}_0| + \sum_{l=1}^{m-1} \left( 1 + \left( 1 - \frac{l}{M} \right)^{-s} \right) \mathbb{1}_n |\bar{Q}_{l,1} + i\bar{Q}_{l,2}|$$

so that

$$|f_k(\bar{x})|_\infty \leq k^{-s} \|\mathcal{A}\|_{s^*} |W|_\infty, \quad \text{for } k \geq M.$$

Finally, using  $\|\Lambda_k^{-1}\|_\infty \leq \frac{C_\Lambda}{M}$ , define

$$Y_M \stackrel{\text{def}}{=} \frac{1}{M^{s+1}} \|\mathcal{A}\|_{s^*} C_\Lambda |W|_\infty. \quad (26)$$

### 2.5.2 The bound $Z$

To construct the bound  $Z$  satisfying

$$\sup_{b_1, b_2 \in B(r)} \left| [DT(\bar{x} + b_1)b_2]_k \right| \leq_{cw} Z_k(r), \quad \forall k \geq 0,$$

it is convenient to factor the points  $b_1, b_2 \in B(r)$  as  $b_1 = ru, b_2 = rv$  with  $u, v \in B(1)$ , to expand in the variable  $r$  and finally to uniformly bound the expression using the fact that  $u, v \in B(1)$ . Denote  $u = [u_0, u_1, \dots, u_k, \dots]$ , where each  $u_k = (u_{k,1}, u_{k,2}) \in Mat(n, \mathbb{R})^2$ . In order to simplify the exposition, both the matrices  $u_{k,1}, u_{k,2}$  will be denoted as  $u_k$ . Indeed, what really matters is the bound  $|u_{k,1}|, |u_{k,2}| \leq_{cw} w_k^{-s}$  that finally will be applied to obtain the uniform estimates. The similar notation for  $v_k$ .

Let us introduce the linear operator  $A^\dagger : \Omega^{s+1} \rightarrow \Omega^s$  defined as

$$(A^\dagger x)_k \stackrel{\text{def}}{=} \begin{cases} (L_M \cdot x^M)_k & k = 0, \dots, M-1 \\ \Lambda_k x_k, & k \geq M, \end{cases} \quad (27)$$

where  $L_M$  is the same as in (14), and consider the splitting

$$\begin{aligned} DT(\bar{x} + ru)rv &= [I - ADf(\bar{x} + ru)]rv \\ &= [I - AA^\dagger]rv - A[Df(\bar{x} + ru) - A^\dagger]rv. \end{aligned} \quad (28)$$

The definition of  $Z(r)$  will follow as a result of different intermediate estimates: indeed we are going to introduce the vectors  $Z^0, Z^1, Z^2$  such that

$$\begin{aligned} |[I - AA^\dagger]rv| &\leq_{cw} Z^0 r, \quad \forall v \in B(1), \\ |[Df(\bar{x} + ru) - A^\dagger]rv| &\leq_{cw} Z^1 r + Z^2 r^2, \quad \forall u, v \in B(1). \end{aligned}$$

From (28) it follows that

$$|[DT(\bar{x} + ru)rv]| \leq_{cw} |[(I - AA^\dagger)rv]| + |[A(Df(\bar{x} + ru) - A^\dagger)rv]|. \quad (29)$$

Hence, the elements  $Z_k$ , for  $k = 0, \dots, M-1$  can be defined as

$$Z_k(r) = Z_k^0 r + [|A_M|(Z^1 r + Z^2 r^2)^M]_k, \quad k = 0, \dots, M-1$$

Finally the element  $Z_M$  will be defined to satisfy (21).

*The bound  $Z_0$*

Since  $|v_k| \leq_{cw} w_k^{-s} \mathbb{1}$ , define  $Z^0$  as

$$(Z^0)_k = \begin{cases} [|I - A_M L_M| \{w_j^{-s} \mathbb{1}\}_{j=0}^{M-1}]_k & k = 0, \dots, M-1 \\ 0, & k \geq M \end{cases} \quad (30)$$

so that

$$|[(I - AA^\dagger)rv]| \leq_{cw} Z^0 r.$$

Note that  $A^\dagger$  is an almost inverse of  $A$ , indeed by definition  $A_M L_M \approx I$ . Then the size of  $Z^0$  is small and depends on the accuracy of the numerical method that computes the inverse  $A_m$ .

*The bounds  $Z^1, Z^2$*

Concerning the terms in  $Z^1, Z^2$ , consider the expansion as quadratic polynomial in  $r$

$$[(Df(\bar{x} + ru) - A^\dagger) rv]_k = \sum_{i=1,2} c_{k,i} r^i. \quad (31)$$

First note that

$$(A \cdot Q)_{k,1} = \sum_{k_1+k_2=k} \left( Re(\mathcal{A}_{k_1}) Q_{k_2,1} - Im(\mathcal{A}_{k_1}) Q_{k_2,2} \right),$$

$$(A \cdot Q)_{k,2} = \sum_{k_1+k_2=k} \left( Im(\mathcal{A}_{k_1}) Q_{k_2,1} + Re(\mathcal{A}_{k_1}) Q_{k_2,2} \right),$$

then, taking in mind that  $Q_{k,2} = -Q_{-k,2}$  and denoting with  $sg(l) = \text{sign}(l)$ , one computes

$$c_{0,1} = \begin{bmatrix} 2 \sum_{k \geq M} v_k, \\ - \sum_{\substack{k_1+k_2=0 \\ |k_2| \geq m}} \left( Re(\mathcal{A}_{k_1}) - sg(k_2) Im(\mathcal{A}_{k_1}) \right) v_{|k_2|} \end{bmatrix}, \quad c_{0,2} = \begin{bmatrix} 0 \\ u_0 v_0 + v_0 u_0 \end{bmatrix}, \quad (32)$$

for  $k = 1, \dots, m-1$

$$c_{k,1} = - \sum_{\substack{k_1+k_2=k \\ |k_2| \geq m}} \begin{bmatrix} \left( Re(\mathcal{A}_{k_1}) - sg(k_2) Im(\mathcal{A}_{k_1}) \right) v_{|k_2|} \\ \left( Im(\mathcal{A}_{k_1}) + sg(k_2) Re(\mathcal{A}_{k_1}) \right) v_{|k_2|} \end{bmatrix}, \quad c_{k,2} = \begin{bmatrix} u_k v_0 + v_k u_0 \\ u_k v_0 + v_k u_0 \end{bmatrix}, \quad (33)$$

and for  $k \geq m$

$$c_{k,1} = - \sum_{\substack{k_1+k_2=k \\ |k_2| \neq k}} \begin{bmatrix} \left( Re(\mathcal{A}_{k_1}) - sg(k_2) Im(\mathcal{A}_{k_1}) \right) v_{|k_2|} \\ \left( Im(\mathcal{A}_{k_1}) + sg(k_2) Re(\mathcal{A}_{k_1}) \right) v_{|k_2|} \end{bmatrix}, \quad c_{k,2} = \begin{bmatrix} u_k v_0 + v_k u_0 \\ u_k v_0 + v_k u_0 \end{bmatrix}. \quad (34)$$

Therefore  $Z^1, Z^2$  need to be defined so that  $Z_k^1 \geq_{cw} |c_{k,1}|$  and  $Z_k^2 \geq_{cw} |c_{k,2}|$ , for any  $0 \leq k \leq M-1$ . To achieve this, it is enough to substitute in the above expression the bounds  $|u_k|, |v_k| \leq_{cw} w_k^{-s} \mathbb{1}_n$  and  $|\pm Re(\mathcal{A}_j) \pm Im(\mathcal{A}_j)| \leq_{cw} |Re(\mathcal{A}_j)| + |Im(\mathcal{A}_j)|$ . Since  $\mathbb{1}_n \mathbb{1}_n = n \mathbb{1}_n$ , one gets

$$\begin{aligned} |c_{0,2}| &\leq_{cw} 2n \begin{bmatrix} 0 \\ \mathbb{1}_n \end{bmatrix} =: Z_0^2, \\ |c_{k,2}| &\leq_{cw} 2n w_k^{-s} \begin{bmatrix} \mathbb{1}_n \\ \mathbb{1}_n \end{bmatrix} =: Z_k^2, \quad k \geq 1. \end{aligned} \quad (35)$$

Consider matrices  $H_k$  so that

$$\begin{aligned} |c_{0,1}| &\leq_{cw} \left[ \sum_{\substack{k_1+k_2=0 \\ m \leq |k_2| < M}} \left( |Re(\mathcal{A}_{k_1})| + |Im(\mathcal{A}_{k_1})| \right) w_{k_2}^{-s} \mathbb{1}_n \right] + H_0 =: Z_0^1 \\ |c_{k,1}| &\leq_{cw} \sum_{\substack{k_1+k_2=k \\ m \leq |k_2| < M}} \left[ \begin{array}{l} \left( |Re(\mathcal{A}_{k_1})| + |Im(\mathcal{A}_{k_1})| \right) w_{k_2}^{-s} \mathbb{1}_n \\ \left( |Im(\mathcal{A}_{k_1})| + |Re(\mathcal{A}_{k_1})| \right) w_{k_2}^{-s} \mathbb{1}_n \end{array} \right] + H_k =: Z_k^1, \quad k = 1, \dots, m-1 \\ |c_{k,1}| &\leq_{cw} \sum_{\substack{k_1+k_2=k \\ |k_2| \neq k, |k_2| < M}} \left[ \begin{array}{l} \left( |Re(\mathcal{A}_{k_1})| + |Im(\mathcal{A}_{k_1})| \right) w_{k_2}^{-s} \mathbb{1}_n \\ \left( |Im(\mathcal{A}_{k_1})| + |Re(\mathcal{A}_{k_1})| \right) w_{k_2}^{-s} \mathbb{1}_n \end{array} \right] + H_k =: Z_k^1, \quad k = m, \dots, M-1. \end{aligned} \tag{36}$$

It means that the bound  $Z^1$  has been defined as sum of two factors: the first obtained by rigorous computation of a finite number of elements in the series, the second analytically defined to estimate the tail parts of the series that have not been computed.

For any  $q > 0, p > 1$ , define the function

$$\zeta(q, p) \stackrel{\text{def}}{=} \frac{1}{(q)^p} + \frac{1}{(q+1)^p} + \frac{1}{p-1} \frac{1}{(q+1)^{p-1}},$$

and

$$H_0 \stackrel{\text{def}}{=} \begin{bmatrix} 2\zeta(M, s)\mathbb{1}_n \\ h_0\mathbb{1}_n \end{bmatrix}, \quad H_k \stackrel{\text{def}}{=} h_k \begin{bmatrix} \mathbb{1}_n \\ \mathbb{1}_n \end{bmatrix}, \tag{37}$$

where for  $k \geq 0$

$$h_k = \frac{\sqrt{2}n\|\mathcal{A}\|_{s^*}}{(M-k)^{s^*-s}} \left( \sum_{k_2=M-k}^{M-1} w_{k_2+k}^{-s} w_{k_2}^{-s} + 2\zeta(M, 2s) \right). \tag{38}$$

Hence, one has the following result.

**Lemma 2.7.** *Formula (36) holds for  $H_0, H_k$  defined in (37).*

*Proof.* First note that for any  $M \geq 1$  and  $s \geq 2$

$$\sum_{k=M}^{\infty} \frac{1}{k^s} < \zeta(M, s). \tag{39}$$

That can be seen from the fact that  $\sum_{k=M}^{\infty} \frac{1}{k^s} = \frac{1}{(M)^s} + \frac{1}{(M+1)^s} + \sum_{k=M+2}^{\infty} \frac{1}{k^s} < \frac{1}{(M)^s} + \frac{1}{(M+1)^s} + \int_{M+1}^{\infty} k^{-s} dk$ . Hence, one has that

$$\left| 2 \sum_{k=M}^{\infty} w_k^{-s} \mathbb{1}_n \right| \leq_{cw} 2\zeta(M, s)\mathbb{1}_n.$$

proving the lemma for the upper half of  $H_0$ . For the remaining terms note that  $(|Re(\mathcal{A}_{k_1})| + |Im(\mathcal{A}_{k_1})|) \leq_{cw} \sqrt{2}|\mathcal{A}_{k_1}| \leq_{cw} \sqrt{2}\frac{\|\mathcal{A}\|_{s^*}}{w_{k_1}^{s^*}}\mathbb{1}_n$ , then, for any  $k \geq 0$ , the tail part of the series can be bounded by

$$\left| \sum_{\substack{k_1+k_2=k \\ |k_2| \geq M}} \left( |Re(\mathcal{A}_{k_1})| + |Im(\mathcal{A}_{k_1})| \right) w_{k_2}^{-s} \mathbb{1}_n \right| \leq_{cw} \sqrt{2}\|\mathcal{A}\|_{s^*} \sum_{k_2=M}^{\infty} \left( \frac{1}{w_{k-k_2}^{s^*}} + \frac{1}{w_{k+k_2}^{s^*}} \right) \mathbb{1}_n w_{k_2}^{-s} \mathbb{1}_n$$

$$\leq_{cw} \frac{\sqrt{2}n\|\mathcal{A}\|_{s^*}}{(M-k)^{s^*-s}} \sum_{k_2=M}^{\infty} \left( \frac{1}{w_{k_2-k}^s} + \frac{1}{w_{k+k_2}^s} \right) w_{k_2}^{-s} \mathbb{1}_n.$$

In the last passage we have used the fact that  $s^* \geq s$  and the relation  $\mathbb{1}_n \mathbb{1}_n = n \mathbb{1}_n$ . The result follows by applying (39) once the last series has been rewritten as

$$\begin{aligned} \sum_{k_2=M}^{\infty} \left( \frac{1}{w_{k_2-k}^s} + \frac{1}{w_{k+k_2}^s} \right) w_{k_2}^{-s} &= \sum_{k_2=M}^{\infty} \left( \frac{1}{w_{k+k_2}^s} \right) w_{k_2}^{-s} + \sum_{k_2=M-k}^{\infty} \left( \frac{1}{w_{k+k_2}^s} \right) w_{k_2}^{-s} \\ &\leq \sum_{k_2=M-k}^{\infty} w_{k+k_2}^{-s} w_{k_2}^{-s} + 2 \sum_{k_2=M}^{\infty} w_{k_2}^{-2s}. \end{aligned} \quad (40)$$

■

*The bound  $Z_M$*

From [10], one has that for  $k \geq M$ ,

$$\sum_{\substack{k_1+k_2=k \\ |k_1| \neq k}} \frac{1}{w_{k_1}^s w_{k_2}^s} \leq \frac{1}{w_k^s} \left[ 1 + 2 \sum_{l=1}^M \frac{1}{l^s} + \frac{2}{M^{s-1}(s-1)} + \eta_M - \frac{1}{w_{2k}^s} \right],$$

where

$$\eta_k = 2 \left[ \frac{k}{k-1} \right]^s + \left[ \frac{4 \log(k-2)}{k} + \frac{\pi^2 - 6}{3} \right] \left[ \frac{2}{k} + \frac{1}{2} \right]^{s-2}.$$

Recall the definition of  $c_{k,1}$  and  $c_{k,2}$  given in (31), with a more explicit form in (34) for the case  $k \geq m$ . Then for  $k \geq M$  one has that

$$\begin{aligned} |c_{k,1}|_\infty &\leq \sqrt{2}n\|\mathcal{A}\|_{s^*} \sum_{\substack{k_1+k_2=k \\ |k_2| \neq k}} \frac{1}{w_{k_1}^{s^*} w_{k_2}^s} \leq \sqrt{2}n\|\mathcal{A}\|_{s^*} \sum_{\substack{k_1+k_2=k \\ |k_2| \neq k}} \frac{1}{w_{k_1}^s w_{k_2}^s} \\ &\leq \frac{\sqrt{2}n\|\mathcal{A}\|_{s^*}}{w_k^s} \left[ 1 + 2 \sum_{l=1}^M \frac{1}{l^s} + \frac{2}{M^{s-1}(s-1)} + \eta_M \right] =: \frac{\sqrt{2}n\|\mathcal{A}\|_{s^*}}{w_k^s} C_1, \\ |c_{k,2}|_\infty &\leq \frac{2n}{w_k^s}. \end{aligned}$$

Since for  $k \geq M$  the first term on the right hand side of (29) is zero, the following estimate holds

$$\begin{aligned} \left| [DT(\bar{x} + ru)rv]_k \right|_\infty &\leq_{cw} \left| [A(Df(\bar{x} + ru) - A^\dagger)rv]_k \right|_\infty \\ &\leq \|\Lambda_k^{-1}\|_\infty (|c_{k,1}|_\infty r + |c_{k,2}|_\infty r^2). \end{aligned} \quad (41)$$

Finally, combining (23) and that  $k \geq M$ , one gets that  $\|\Lambda_k^{-1}\|_\infty \leq \frac{C_\Lambda}{M}$ , and we can define  $Z_M$

$$Z_M = \frac{C_\Lambda}{M^s} (\sqrt{2}\|\mathcal{A}\|_{s^*} C_1 r + 2nr^2).$$

**Remark 2.8.** We remark that the above quantities  $h_k$ ,  $Z_M$  as like as  $Y_M$  given in (26) depend on the  $s^*$ -norm of the sequence of the Fourier coefficients of  $A(t)$ , defined in (10). Since the only assumption we made on the Fourier coefficients  $A_k$  is  $\|\mathcal{A}\|_{s^*} < \infty$  we did not stress how to improve the estimates. However it is easy to see that formulas (26) and (38) can be

rewritten respectively with the quantities  $\sup_{j \geq M-m} \{|\mathcal{A}_j|_\infty w_j^{s^*}\}$  and  $\sup_{|j| \geq M-k} \{|\mathcal{A}_j|_\infty w_j^{s^*}\}$  in place of  $\|\mathcal{A}\|_{s^*}$ . Therefore, a more detailed knowledge of the behavior of the coefficients  $\mathcal{A}_k$  should suggest the choice of the computational parameter  $M$  in order to improve the estimates. For instance, assume that  $|\mathcal{A}_k|_\infty w_k^{s^*} < \varepsilon$  for any  $|k| > m_{\mathcal{A}}$ : then, setting  $M > m + m_{\mathcal{A}}$  the estimate (26) holds with  $\varepsilon$  in place of  $\|\mathcal{A}\|_{s^*}$ .

### 3 Computing stable and unstable bundles of periodic orbits via Floquet normal forms

Consider an autonomous differential equation

$$\dot{y} = g(y), \quad g \in C^1(\mathbb{R}^n) \quad (42)$$

and suppose that  $\gamma(t)$  is a  $\tau$ -periodic solution with  $\gamma(0) = \gamma_0$ . Denote by  $\Gamma = \{\gamma(t), t \in [0, \tau]\}$  the support of  $\gamma$  and for any  $\theta \in [0, \tau]$ , define  $\gamma_\theta(t) = \gamma(t + \theta)$  the phase-shift re-parametrization of  $\Gamma$ . Being autonomous, system (42) has the property that any of the curves  $\gamma_\theta(t)$  is a  $\tau$ -periodic solution satisfying  $\gamma_\theta(0) = \gamma(\theta)$ . We refer to  $\Gamma$  as the periodic orbit and  $\gamma_\theta$  as the periodic solutions.

**Definition 3.1** (Monodromy matrix). Let  $\gamma : \mathbb{R} \rightarrow \mathbb{R}^n$  be a  $\tau$ -periodic solution (42) and let  $\Phi_\theta(t)$  be the unique solution of the non-autonomous linear problem

$$\begin{cases} \dot{\Phi}_\theta = \nabla g(\gamma_\theta(t))\Phi_\theta \\ \Phi_\theta(0) = I. \end{cases} \quad (43)$$

The matrix  $\Phi_\theta(\tau)$  is called the *monodromy matrix* of  $\gamma_\theta(t)$ .

Having chosen  $\gamma(t) = \gamma_0(t)$ , in the following we identify  $\Phi(\tau) = \Phi_0(\tau)$ . The next two Lemmas are classical results and are direct consequence of  $\Phi_\theta(t)$  being a fundamental matrix solution. For sake of completeness, we present their proofs.

**Lemma 3.2.** *For any  $\theta \in [0, \tau]$ , the solution  $\Phi_\theta(t)$  of (42) satisfies*

$$\Phi_\theta(n\tau + t) = \Phi_\theta(t)\Phi_\theta(\tau)^n, \quad \forall t \in \mathbb{R}, \quad \forall n \in \mathbb{N}.$$

*Proof.* Without loss of generality let us consider  $\theta = 0$ . By induction on  $n \geq 0$ . For  $n = 0$  the result is obvious. Suppose it holds for  $n - 1$ . Then

$$\Phi(n\tau) = \Phi((n-1)\tau + \tau) = \Phi(\tau)\Phi(\tau)^{n-1} = \Phi(\tau)^n.$$

Define

$$\Psi(t) = \Phi(t + n\tau)\Phi(n\tau)^{-1}.$$

It follows that  $\Psi(0) = I$  and that

$$\dot{\Psi}(t) = \dot{\Phi}(n\tau + t)\Phi(n\tau)^{-1} = A(n\tau + t)\Phi(n\tau + t)\Phi(n\tau)^{-1} = A(t)\Psi(t)$$

For the uniqueness of solutions of the initial value problem,  $\Psi(t) = \Phi(t)$  thus

$$\Phi(t + n\tau) = \Phi(t)\Phi(n\tau) = \Phi(t)\Phi(\tau)^n, \quad \forall t \in \mathbb{R}.$$

■

**Lemma 3.3.** *The matrices  $\Phi_\theta(\tau)$  are equivalent under conjugation. In particular*

$$\Phi_\theta(\tau) = \Phi(\theta)\Phi(\tau)\Phi(\theta)^{-1}. \quad (44)$$

*Proof.* The matrix  $\tilde{\Phi}(t)$  by def  $\Phi(t + \theta)$  is solution of the equation  $\dot{y} = \nabla g(\gamma(t + \theta))y = \nabla g(\gamma_\theta(t))$ , with  $\tilde{\Phi}(0) = \Phi(\theta)$ . Since  $\Phi_\theta(t)$  is the principal fundamental solution of the previous system,

$$\tilde{\Phi}(t) = \Phi_\theta(t)\Phi(\theta).$$

It follows

$$\Phi_\theta(t) = \tilde{\Phi}(t)\Phi(\theta)^{-1} = \Phi(t + \theta)\Phi(\theta)^{-1}, \quad \forall t. \quad (45)$$

Thus

$$\Phi_\theta(\tau) = \Phi(\tau + \theta)\Phi(\theta)^{-1} = \Phi(\theta)\Phi(\tau)\Phi(\theta)^{-1}$$

where, in the last passage, Lemma 3.2 has been used.  $\blacksquare$

The previous result implies that all monodromy matrices  $\Phi_\theta(\tau)$  have the same eigenvalues. That motivates the following definition.

**Definition 3.4.** The eigenvalues  $\sigma_j$  of the monodromy matrix  $\Phi(\tau)$  are called the *Floquet multipliers* of the periodic orbit  $\Gamma$ .

As already mentioned in Section 1, in the theory of dynamical systems the monodromy matrix  $\Phi(\tau)$  associated to a periodic solution  $\gamma(t)$  plays a fundamental role since it encompasses the information about the stability character of  $\gamma$ . Indeed, as shown in Proposition 2.122 in [2], the Floquet multipliers of  $\gamma(t)$  are in fact the eigenvalues of  $D\mathbf{P}(\gamma(0))$ , where  $\mathbf{P}(x)$  denotes the Poincaré map of  $\gamma(t)$  on a  $(n-1)$ -dimensional hypersurface transversal to  $\gamma$  at  $\gamma(0)$ . Moreover, it can be proved that at least one of the Floquet multipliers  $\sigma_j$  of  $\Phi(\tau)$  is equal to one, corresponding to the eigenvector  $\dot{\gamma}(0)$ . Hence, we will denote by  $\sigma_n = 1$  the Floquet multiplier corresponding to  $\dot{\gamma}(0)$  and denote by  $\{\sigma_j\}_{j=1,\dots,n-1}$  the set of non trivial Floquet multipliers. We refer to Section 2.4 in [2] for a more extensive analysis of the links between Poincaré sections and Floquet theory. Based on the above discussion, we are now ready to introduce the definition of stability of a periodic orbit.

**Definition 3.5.** Let  $\Gamma = \{\gamma(t), t \in [0, \tau]\}$  be a  $\tau$ -periodic orbit of the system (42) and let  $\{\sigma_j\}_{j=1,\dots,n-1}$  be the corresponding set of non trivial Floquet multipliers. We say that

- $\Gamma$  is *stable* if  $\forall j \in \{1, \dots, n-1\}$ ,  $|\sigma_j| < 1$ ;
- $\Gamma$  is *unstable* if  $\exists j \in \{1, \dots, n-1\}$  such that  $|\sigma_j| > 1$ .

Moreover, if  $p < n-1$  Floquet multipliers have modulus less than one, and  $q < n-p$  Floquet multipliers have modulus greater than one,  $\Gamma$  is said to have  $p$  stable directions and  $q$  unstable directions.

Let us mention that there is a variant to the Floquet normal form introduce in Theorem 1.1, namely there exist a constant (possibly complex) matrix  $B$  and a nonsingular (possibly complex) continuously differentiable,  $\tau$ -periodic matrix function  $P(t)$  such that  $\Phi(t) = P(t)e^{Bt}$ . We refer to Theorem 2.83 in [2] for more details and for the proof. Therefore, there exists a (possibly complex) matrix  $B$  such that  $\Phi(\tau) = e^{B\tau}$ . Denoting by  $\lambda_j$  the eigenvalues of  $B$ , it follows that  $\sigma_j = e^{\tau\lambda_j}$  is a Floquet multiplier. Note that for a given  $\sigma_j$ , the solution  $\lambda_j$  of  $\sigma_j = e^{\tau\lambda_j}$  is not uniquely defined. Indeed for any  $k \in \mathbb{Z}$ ,  $e^{\tau(\lambda_j + i\frac{2k\pi}{\tau})} = \sigma_j$ . This reflects the fact that in the *complex Floquet normal form*  $\Phi(t) = P(t)e^{Bt}$ , the matrix  $B$  is also not uniquely defined. In the literature it is common to call a Floquet exponent associated to  $\sigma_j$  any complex number  $\lambda_j$  so that  $\sigma_j = e^{\tau\lambda_j}$ . On the converse, for any  $\sigma_j$  there is a unique real number  $l_j$  so that  $|\sigma_j| = e^{l_j\tau}$ . That motivates the following definition.

**Definition 3.6.** A Lyapunov exponent associated to a Floquet multiplier  $\sigma_j$  is the unique real number  $l_j$  so that  $|\sigma_j| = e^{l_j \tau}$ .

Note that using the notion Lyapunov exponents, a definition of stability of a periodic orbit similar to the one of Definition 3.5 can be introduced. Indeed, given a  $\tau$ -periodic orbit  $\Gamma = \{\gamma(t), t \in [0, \tau]\}$  of (42) and considering  $\{l_j\}_{j=1, \dots, n-1}$  to be the corresponding set of non trivial Lyapunov exponents, we say that  $\Gamma$  is stable if  $l_j < 0, \forall j = 1, \dots, n-1$  and that  $\Gamma$  is unstable if there exists  $j \in \{1, \dots, n-1\}$  such that  $l_j > 0$ .

Given a real  $n \times n$  diagonalizable matrix  $A$ , let us introduce the notation  $\Sigma(A) = \{\alpha_k, v_k\}_{k=1, \dots, n}$  to denote the eigendecomposition of the square matrix  $A$ , i.e.  $Av_k = \alpha_k v_k$ , for all  $k = 1, \dots, n$ .

The following result shows how the information from the couple  $(R, Q(t))$  coming from the Floquet normal form  $\Phi(t) = Q(t)e^{Rt}$  can directly be used to study the dynamical properties of the periodic orbit  $\Gamma$ . More explicitly, it demonstrates that the stability of  $\Gamma$  can be determined by the eigenvalues of  $R$  while the stable and unstable tangent bundles of  $\Gamma$  can be retrieved from the action of  $Q(t)$  (with  $t \in [0, \tau]$ ) on the eigenvectors of  $R$ .

**Theorem 3.7.** Assume that  $\Gamma = \{\gamma(t), t \in [0, \tau]\}$  is a  $\tau$ -periodic orbit of (42) and consider  $\Phi(t)$  the fundamental matrix solution of the non-autonomous linear equation  $\dot{y} = \nabla g(\gamma(t))y$  such that  $\Phi(0) = I$ . Suppose that a Floquet normal form decomposition of Theorem 1.1)  $\Phi(t) = Q(t)e^{Rt}$  is known. Assume that the real  $n \times n$  matrix  $R$  is diagonalizable and let  $\Sigma(R) = \{\mu_j, v_j\}_{j=1, \dots, n}$  the eigendecomposition of  $R$ . Then the Lyapunov exponents  $l_j$  of  $\Gamma$  are given by

$$l_j = \operatorname{Re}(\mu_j). \quad (46)$$

Furthermore, for any  $\theta \in [0, \tau]$ , if one defines

$$w_j^\theta \stackrel{\text{def}}{=} Q(\theta)v_j, \quad (47)$$

then  $w_j^\theta$  is an eigenvector of  $\Phi_\theta(\tau)$  associated to the Lyapunov exponent  $l_j$ . Note that  $w_j^\theta$  is a smooth  $2\tau$ -periodic function of  $\theta$ .

*Proof.* Consider the eigendecomposition  $\Sigma(R) = \{\mu_j, v_j\}_{j=1, \dots, n}$  of the diagonalizable matrix  $R$ , meaning that the set  $\{v_1, \dots, v_n\}$  consists of  $n$  linearly independent eigenvectors of  $R$ . By Lemma 3.2, one has that  $\Phi(\tau)^2 = \Phi(2\tau)$ . Since  $Q(t)$  is  $2\tau$ -periodic and  $Q(0) = I$ , it follows that  $\Phi(2\tau) = e^{R2\tau}$ . Since  $R$  is diagonalizable,  $\Phi(2\tau) = e^{R2\tau}$  is also diagonalizable. Since  $\Phi(2\tau) = \Phi(\tau)^2$  and since the matrix  $\Phi(\tau)$  is invertible and defined over the field of complex number (which has zero characteristic), then it can then be showed that  $\Phi(\tau)$  is also diagonalizable. Now, since  $\Phi(2\tau) = \Phi(\tau)^2$  one has that if  $(\sigma, w) \in \Sigma(\Phi(\tau))$ , then  $(\sigma^2, w) \in \Sigma(\Phi(2\tau))$ . Combining this last point with  $\Phi(\tau), \Phi(2\tau)$  being diagonalizable implies that the eigenspaces of  $\Phi(\tau)$  and  $\Phi(2\tau)$  are in one-to-one correspondence. That implies the existence of a set  $\{\sigma_j\}_{j=1, \dots, n}$  such that  $\Sigma(\Phi(\tau)) = \{\sigma_j, v_j\}_{j=1, \dots, n}$ . From the property of the exponential matrix operator,  $\Sigma(\Phi(2\tau)) = \{e^{\mu_j 2\tau}, v_j\}_{j=1, \dots, n} = \Sigma(\Phi(\tau)^2) = \{\sigma_j^2, v_j\}_{j=1, \dots, n}$ . This implies that  $\sigma_j^2 = e^{\mu_j 2\tau}$  for any  $j = 1, \dots, n$ . Note that  $l_j = \operatorname{Re}(\mu_j)$  is the unique real number so that  $|\sigma_j| = e^{l_j \tau}$ . Hence,  $l_j$  is a Lyapunov exponent associated to the Floquet multipliers  $\sigma_j$ .

Now, from (45), one has that

$$\Phi_\theta(2\tau) = \Phi(2\tau + \theta)\Phi(\theta)^{-1} = Q(\theta)e^{(2\tau+\theta)R}e^{-R\theta}Q(\theta)^{-1}, \quad \forall \theta \in [0, \tau]$$

thus

$$\Phi_\theta(2\tau)Q(\theta)v_j = Q(\theta)e^{2\tau R}v_j = e^{2\tau \mu_j}Q(\theta)v_j$$

showing that  $\Sigma(\Phi_\theta(2\tau)) = \{e^{2\tau\mu_j}, Q(\theta)v_j\}$ . Applying the same argument than above, one can conclude that  $\Sigma(\Phi_\theta(\tau)) = \{\sigma_j, Q(\theta)v_j\}_{j=1,\dots,n}$  forms an eigendecomposition of the matrix  $\Phi_\theta(\tau)$ . Hence,  $w_j^\theta = Q(\theta)v_j$  is an eigenvector of  $\Phi_\theta(\tau)$ . By the smoothness and the  $2\tau$ -periodicity of the matrix function  $Q(\theta)$ , one can conclude that  $w_j^\theta = Q(\theta)v_j$  is also a smooth  $2\tau$ -periodic function of  $\theta$ .  $\blacksquare$

Recall (47) and consider  $w_j^\theta = a_j^\theta + ib_j^\theta$ . We define the stable and unstable subspaces  $E_s^\theta, E_u^\theta \subset T_{\gamma(\theta)}\mathbb{R}^n$  of the periodic orbit  $\Gamma$  at the point  $\gamma(\theta)$  as

$$E_s^\theta = \text{Span}\{a_i^\theta, b_i^\theta : |\sigma_j| < 0\}$$

$$E_u^\theta = \text{Span}\{a_i^\theta, b_i^\theta : |\sigma_j| > 0\}.$$

That allows us to define the following

**Definition 3.8.** We define the *stable* and *unstable tangent bundles* of  $\Gamma$  respectively by

$$E_s, E_u \subset T_\Gamma\mathbb{R}^n$$

$$E_s = \bigcup_{\theta \in [0, \tau]} \{\gamma(\theta)\} \times E_s^\theta, \quad E_u = \bigcup_{\theta \in [0, \tau]} \{\gamma(\theta)\} \times E_u^\theta.$$

It is important to remark that from the conclusion of Theorem 3.7, the complete structure of the stable and unstable bundles can be recovered by the action of the matrix function  $Q(t)$  on the eigenvectors of  $R$ , which themselves correspond to the stable and unstable directions at the point  $\gamma(0)$  on  $\Gamma$ . Also, the proof of Theorem 3.7 is constructive in the sense that combined with the rigorous computational method of Section 2, it provides a computationally efficient direct way to obtain the eigenvectors  $w_j^\theta$  of  $\Phi_\theta(\tau)$ , which are the ingredients defining the bundles of Definition 3.8. Note that one could be tempted to use the fact that  $\Phi(\tau) = Q(\tau)e^{R\tau}$  and then attempt to compute the eigendecomposition of  $\Phi(\tau)$  directly. However, that would imply having to compute the exponential of an interval valued matrix, which turns out to be a difficult task (e.g. see [12], [13]). This being said, the rigorous computation of the eigendecomposition of the interval matrix  $R$  is not completely straightforward. We addressed this problem by adapting the computational method based on the radii polynomials in order to enclose all the solution  $\{\mu_k, v_k\}$  of the nonlinear problem  $(R - \mu I)v = 0$  with some scaling constrain to isolate the solution. Further details on the enclosure of the eigendecomposition of interval matrices is presented in [14].

## 4 Applications

In this section, we present some applications, where we construct rigorously tangent stable and unstable bundles of some periodic orbits of the Lorenz equations in Section 4.1 and of the  $\zeta^3$ -model in Section 4.2. Finally, in Section 4.3, we discuss how to recover a posteriori the Floquet multipliers associated to the periodic orbit  $\gamma(t)$ , that is the eigenvalues of the matrices  $\Phi_\theta(\tau)$ . Note that all rigorous computations were performed in *Matlab* with the interval arithmetic package *Intlab* [15], while the codes necessary to compute the Floquet normal forms in the context of the Lorenz equations can be found in [19].

## 4.1 Bundles of periodic orbits in the Lorenz equations

Consider the following three dimensional system of ODEs, known as the Lorenz equations

$$\begin{cases} \dot{u}_1 = \sigma(u_2 - u_1) \\ \dot{u}_2 = \rho u_1 - u_2 - u_1 u_3 \\ \dot{u}_3 = u_1 u_2 - \beta u_3 \end{cases} \quad (48)$$

with the classical choice of parameters  $\beta = 8/3$ ,  $\sigma = 10$  and  $\rho$  left as a bifurcation parameter. First we rigorously compute a family of periodic solutions  $\gamma(t) = [\gamma^1, \gamma^2, \gamma^3](t)$  of (48) in the form

$$\gamma^j(t) = \sum_{k \in \mathbb{Z}} \xi_k^j e^{ik\frac{2\pi}{\tau_\gamma} t}, \quad j = 1, 2, 3 \quad (49)$$

one of each in a ball of radius  $r_\gamma$ , with respect to the  $\Omega^{s^*}$  norm, around a numerical solution  $[\bar{\tau}_\gamma, \bar{\xi}_k]$ ,  $\bar{\xi}_k = 0$  for  $|k| > m_\gamma$ . More explicitly, for a choice of the parameter  $\rho$  and a decay rate  $s^* \geq 2$ , we prove the existence of a  $\tau_\gamma$ -periodic solution  $\gamma(t)$  so that

$$\begin{aligned} |\tau_\gamma - \bar{\tau}_\gamma| &\leq r_\gamma, \\ |Re(\xi_k) - Re(\bar{\xi}_k)|_\infty &\leq r_\gamma w_k^{-s^*}, \quad |Im(\xi_k) - Im(\bar{\xi}_k)|_\infty \leq r_\gamma w_k^{-s^*}. \end{aligned} \quad (50)$$

Note that  $\xi_k \in \mathbb{C}^3$  and  $\xi_{-k} = \mathcal{C}(\xi_k)$ , where  $\mathcal{C}(z)$  is the complex conjugate of  $z$ . The existence of such solutions has been achieved by applying a modified version of the method discussed in the previous section. Even with some technical differences, the philosophy is the same. Rewrite the system of ODEs as a infinite dimensional algebraic system where  $\tau_\gamma$  and the Fourier coefficients  $\xi_k$  are the unknowns, then consider a finite dimensional projection and compute a numerical approximate solution  $\bar{\tau}_\gamma, (\bar{\xi}_k)_k$ . Then, using the radii polynomials, prove the existence, in a suitable Banach space, of a genuine solution  $\tau_\gamma, (\xi_k)_k$  of the infinite dimensional problem in a small ball containing the approximate solution. In the next subsection some of the results are presented.

Then, combining the method discussed in Section 2 and Theorem 3.7, we rigorously enclose the stable and unstable tangent bundles of some of the rigorously computed periodic orbits  $\gamma(t)$ . This first requires the computation of the Floquet normal form of the principal fundamental matrix solution  $\Phi(t)$  of the linearized system along  $\gamma(t)$ . More explicitly  $\Phi(t)$  is the solution for  $t \in [0, \tau_\gamma]$  of the non-autonomous system

$$\begin{cases} \dot{\Phi} = \nabla g(\gamma(t))\Phi \\ \Phi(0) = I \end{cases} \quad (51)$$

where  $g$  is the right hand side of (48),  $\nabla g$  denotes the Jacobian of the right hand side of system (48) and  $I$  is the  $3 \times 3$  identity matrix. The former system is nothing more than a particular case of (1), where  $A(t) = \nabla g(\gamma(t))$  and  $n = 3$ . We now apply the computational method presented in Section 2 to compute the Floquet normal form of  $\Phi(t)$ , which is the solution of (51). In particular a constant matrix  $R$  and the Fourier coefficients  $Q_k$  of a  $2\tau_\gamma$ -periodic function  $Q(t)$  will be computed, so that  $\Phi(t) = Q(t)e^{Rt}$  solves (51). Once the computation of  $R$  and the  $Q_k$  is done, following the conclusion of Theorem 3.7, we compute  $\Sigma(R) = \{(\mu_j, v_j) \mid j = 1, \dots, n\}$ , we derive from the Lyapunov exponents  $l_j \stackrel{\text{def}}{=} Re(\mu_j)$  the linear stability of the periodic orbit  $\Gamma$  and using the eigenvectors  $\{v_1, \dots, v_n\}$  of  $R$  we construct the tangent bundles as defined in Definition 3.8 and given by the formula (47).

### Computation of $R$ and $Q_k$

To begin with, let us explicitly write the Jacobian of (48)

$$\nabla g(u) = \begin{bmatrix} -\sigma & \sigma & 0 \\ \rho - u_3 & -1 & -u_1 \\ u_2 & u_1 & -\beta \end{bmatrix}$$

and, recalling (5), the Fourier coefficients  $\mathcal{A}_k$  of  $A(t) = \nabla g(\gamma(t))$

$$\mathcal{A}_0 = \begin{bmatrix} -\sigma & \sigma & 0 \\ \rho - \xi_0^3 & -1 & -\xi_0^1 \\ \xi_0^2 & \xi_0^1 & -\beta \end{bmatrix}, \quad \mathcal{A}_k = \begin{bmatrix} 0 & 0 & 0 \\ -\xi_k^3 & 0 & -\xi_k^1 \\ \xi_k^2 & \xi_k^1 & 0 \end{bmatrix}, \quad k \geq 1.$$

Note that the hypothesis (50) for  $\xi_k$  to lie in a ball centered at  $\bar{\xi}_k$  implies that  $\|\mathcal{A}\|_{s^*} < \infty$ . The computation of the approximate solution  $\bar{R}, \bar{Q}_{k,1}, \bar{Q}_{k,2}$  has been done as follow: consider the approximation  $\bar{\gamma}(t) = \sum_{|k| \leq m_\gamma} \bar{\xi}_k e^{ik2\pi t/\bar{\tau}_\gamma}$  of the periodic orbit  $\gamma(t)$  and numerically solve system (51) up to time  $2\bar{\tau}_\gamma$ . Denote by  $\bar{y}(2\bar{\tau}_\gamma)$  the obtained result and numerically compute

$$\mathcal{R} = \log(\bar{y}(2\bar{\tau}_\gamma)).$$

Neglect the imaginary part of  $\mathcal{R}$  and consider only its real part. Then numerically integrate the system (3) up to time  $2\bar{\tau}_\gamma$  with  $\mathcal{R}$  in place of  $R$  yielding the solution  $\mathcal{Q}(t)$ . Fix the finite dimensional parameter  $m$  and compute from  $\mathcal{Q}(t)$  the matrices  $\mathcal{Q}_{k,1}, \mathcal{Q}_{k,2}$ , respectively the real and imaginary part of the Fourier coefficients with  $|k| < m$ . Finally the vector  $(\mathcal{R}, \mathcal{Q}_k)$  is considered as starting point for a Newton iteration scheme applied on the finite dimensional projection defined by (11). Denote the output of the iterative process by  $\bar{x} = (\bar{R}, \bar{Q}_k)$ , that is an approximated solution  $f^{(m)}(\bar{x}) \approx 0$  up to a desired accuracy, with  $f^{(m)}$  defined in (11).

Consider  $\Lambda_k$  given by (13). Note that in the case of the three-dimensional vector field (48),  $\Lambda_k$  is a  $6 \times 6$  matrix and one could compute its inverse analytically using the mathematical software *Maple*. After having computed  $\Lambda_k^{-1}$  one needs to check that the chosen  $m$  satisfies  $m > K$  where  $K$  is the same as in Lemma 2.2, otherwise increase  $m$ .

Then, for a choice of  $M$  and  $2 \leq s \leq s^*$  one can compute the coefficients  $Y_k$  and  $Z_k$ ,  $k = 0, \dots, M$  and  $Y_M, Z_M$  as shown in Section 2.5.

In the following, as well as in all the presented computations, we assume

$$M > m + m_\gamma.$$

Although the bound  $\|\mathcal{A}\|_{s^*} < \infty$  is sufficient to proceed with the computational method, we want to deepen what was highlighted in Remark 2.8: it is easy to see that

$$|\mathcal{A}_k|_\infty \leq \sqrt{2}r_\gamma \frac{1}{w_k^{s^*}}, \quad \forall k > m_\gamma \tag{52}$$

thus the above choice of  $M$  implies that the tail elements  $H_0, H_k$  in (36) only contain the terms  $\mathcal{A}_j$  satisfying  $|\mathcal{A}_j|_\infty \leq \sqrt{2}r_\gamma w_j^{-s^*}$ . Therefore the subsequent estimate for  $h_k$  can be improved by replacing  $\|\mathcal{A}\|_{s^*}$  with  $\sqrt{2}r_\gamma$ , giving

$$h_k = \frac{2nr_\gamma}{(M-k)^{s^*-s}} \left( \sum_{k_2=M-k}^{M-1} w_{k_2+k}^{-s} w_{k_2}^{-s} + 2\zeta(M, 2s) \right), \quad \text{for } k = 1, \dots, m-1.$$

On the other hand, for  $k = m, \dots, M-1$  the above estimate does not hold, since  $M$  could be less than  $k + m_\gamma$ . Therefore, for those  $k$  such that  $M > k + m_\gamma$  we continue using

the previous formula for  $h_k$  while for those  $k$  such that  $M \leq k + m_\gamma$  we proceed as follow. Rewrite explicitly (part of) the vector  $H_k$

$$\begin{aligned} H_k &= \sum_{\substack{k_1+k_2=k \\ M \leq |k_2| \leq k+m_\gamma}} \left( |Re(\mathcal{A}_{k_1})| + |Im(\mathcal{A}_{k_1})| \right) w_{k_2}^{-s} \mathbb{1}_n + 2r_\gamma \sum_{\substack{k_1+k_2=k \\ |k_2| > k+m_\gamma}} w_{k_1}^{-s^*} \mathbb{1}_n w_{k_2}^{-s} \mathbb{1}_n \\ &= \sum_{\substack{k_1+k_2=k \\ M \leq |k_2| \leq k+m_\gamma}} \left( |Re(\mathcal{A}_{k_1})| + |Im(\mathcal{A}_{k_1})| \right) w_{k_2}^{-s} \mathbb{1}_n + 2nr_\gamma \sum_{\substack{k_1+k_2=k \\ |k_2| > k+m_\gamma}} w_{k_1}^{-s^*} w_{k_2}^{-s} \mathbb{1}_n \end{aligned} \quad (53)$$

The first is a finite sum and it is rigorously computed while, following (40), the second contribution can be estimated using

$$\begin{aligned} \sum_{\substack{k_1+k_2=k \\ |k_2| > k+m_\gamma}} w_{k_1}^{-s^*} w_{k_2}^{-s} &= \sum_{k_2=k+m_\gamma+1}^{\infty} \left[ \frac{1}{w_{k_2-k}^{s^*}} + \frac{1}{w_{k_2+k}^{s^*}} \right] \frac{1}{k_2^s} \\ &\leq \frac{1}{(m_\gamma + 1)^{s^*-s}} \sum_{k_2>k+m_\gamma} \left[ \frac{1}{w_{k_2-k}^s} + \frac{1}{w_{k_2+k}^s} \right] \frac{1}{k_2^s} \\ &\leq \frac{1}{(m_\gamma + 1)^{s^*-s}} \left[ \sum_{k_2=m_\gamma+1}^{k+m_\gamma} \frac{1}{(k_2+k)^s} \frac{1}{k_2^s} + 2\zeta(k+m_\gamma+1, 2s) \right] \end{aligned} \quad (54)$$

Summarizing, for those  $k \geq m$ ,  $k < M$  such that  $k + m_\gamma > M$ , we define

$$\begin{aligned} H_k = \sum_{\substack{k_1+k_2=k \\ M \leq |k_2| \leq k+m_\gamma}} \left( |Re(\mathcal{A}_{k_1})| + |Im(\mathcal{A}_{k_1})| \right) w_l^{-s} \mathbb{1}_n + \frac{2nr_\gamma}{(m_\gamma + 1)^{s^*-s}} \left[ \sum_{k_2=m_\gamma+1}^{k+m_\gamma} \frac{1}{(k_2+k)^s} \frac{1}{k_2^s} \right. \\ \left. + 2\zeta(k+m_\gamma+1, 2s) \right] \mathbb{1}_n \end{aligned} \quad (55)$$

where, clearly, the dimension of the dynamical system is  $n = 3$ . Again, the knowledge of the particular behavior of the coefficients  $\mathcal{A}_k$  allows to provide a better estimate for  $Z_M$ . Indeed note that  $|Re(\mathcal{A}_k)| \leq_{cw} |Re(\bar{\mathcal{A}}_k)| + w_k^{-s^*} \mathbb{1}_n$ , where  $\bar{\mathcal{A}}_k$  denotes the matrix  $\mathcal{A}_k$  with the entries  $\bar{\xi}$  in place of  $\xi$  and the same holds for  $|Im(\mathcal{A}_k)|$ . It follows that  $|Re(\mathcal{A}_k)|_\infty + |Im(\mathcal{A}_k)|_\infty < \sqrt{2}|\bar{\xi}_k|_\infty + 2r_\gamma w_k^{-s^*}$  for  $1 \leq |k| \leq m_\gamma$  and (52) for  $|k| > m_\gamma$ .

Therefore, the computation of the bound for  $|c_{k,1}|_\infty$  when  $k \geq M$ , necessary for the definition of  $Z_M$ , has been slightly modified as follows.

$$\begin{aligned} |c_{k,1}| &= \left| \sum_{\substack{k_1+k_2=k \\ |k_2| \neq k}} \left( Re(\mathcal{A}_{k_1}) + Im(\mathcal{A}_{k_1}) \right) w_{k_2}^{-s} \mathbb{1}_n \right| \leq_{cw} \sum_{\substack{k_1+k_2=k \\ k_1 \neq 0, 2k}} \left( |Re(\mathcal{A}_{k_1})| + |Im(\mathcal{A}_{k_1})| \right) w_{k_2}^{-s} \mathbb{1}_n \\ &\leq \sum_{\substack{k_1+k_2=k \\ k_1 \neq 0, |k_1| \leq m_\gamma}} \left( |Re(\bar{\mathcal{A}}_{k_1})| + |Im(\bar{\mathcal{A}}_{k_1})| \right) w_{k_2}^{-s} \mathbb{1}_n + 2r_\gamma \sum_{\substack{k_1+k_2=k \\ |k_2| \neq k}} w_{k_1}^{-s^*} w_{k_2}^{-s} \mathbb{1}_n \mathbb{1}_n. \end{aligned} \quad (56)$$

Then, using the fact that  $s^* \geq s$ , for any  $k \geq M$

$$\begin{aligned}
|c_{k,1}|_\infty &\leq_{cw} n\sqrt{2}\sum_{j=1}^{m_\gamma} |\bar{\xi}_j|_\infty (w_{k-j}^{-s} + w_{k+j}^{-s}) + 2nr_\gamma \sum_{\substack{l+j=k \\ |l| \neq k}} w_j^{-s} w_l^{-s} \\
&\leq_{cw} \frac{n}{k^s} \left[ \sqrt{2}\sum_{j=1}^{m_\gamma} |\bar{\xi}_j|_\infty k^s (w_{k-j}^{-s} + w_{k+j}^{-s}) + 2r_\gamma \left[ 1 + 2\sum_{l=1}^M \frac{1}{l^s} + \frac{2}{M^{s-1}(s-1)} + \eta_M \right] \right] \\
&\leq_{cw} \frac{n}{k^s} \left[ \sqrt{2}\sum_{j=1}^{m_\gamma} |\bar{\xi}_j|_\infty \left( \frac{1}{\left(1 - \frac{j}{M}\right)^s} + 1 \right) + 2r_\gamma \left[ 1 + 2\sum_{l=1}^M \frac{1}{l^s} + \frac{2}{M^{s-1}(s-1)} + \eta_M \right] \right]. \tag{57}
\end{aligned}$$

#### 4.1.1 Computational results

For the choice  $\sigma = 10, \beta = 8/3$  it is known that there exists a branch of periodic solutions parametrized by  $\rho$  joining a Hopf bifurcation at  $\rho = \frac{470}{19} \approx 24.736$  and a homoclinic point at  $\rho \approx 13.9265$ , see Figure 1(a). In what follows, we restrict our attention to the periodic solutions lying on this branch. Table 1 presents data about the computer-assisted proofs of existence of several periodic orbits in the form (49) with bounds of the form (50). As mentioned previously, the existence of such solutions are done via the radii polynomials. For each rigorous computation, we fixed  $s^* = 2$ . Each line of Table 1 corresponds to a different solution and reports the value of  $\rho$ , the period  $\bar{\tau}_\gamma$  of the numerical solution, the dimension  $m_\gamma$  of the finite dimensional projection and the radius  $r_\gamma$  of the ball  $B_{\bar{\gamma}}(r_\gamma) = \bar{\gamma} + \prod_{k \geq 0} [-\frac{r_\gamma}{w_k^2}, \frac{r_\gamma}{w_k^2}]^6$  around the numerical solution  $\bar{\gamma}$  where the exact solution has been proved to exist. Some of the periodic orbits are depicted in Figure 1(b). Note that with the radii polynomials, it is possible to rigorously enclose the periodic solutions for values of  $\rho$  very close to the Hopf bifurcation and to the homoclinic point. As  $\rho$  approaches the homoclinic point, the periodic solutions are *flatter* (e.g. see Figure 2), which means that a larger number of Fourier coefficients contributes to their Fourier expansions. Therefore, it is necessary to chose a larger finite dimensional projection  $m_\gamma$  as  $\rho$  decreases in order to obtain rigorous computations of existence of periodic orbits using the radii polynomials.

The rigorous computation of the enclosure of the invariant bundles was done for a set of periodic orbits lying on the same bifurcation branch (see Figure 1(a)), and the corresponding values of  $\rho$  are

$$\rho_1 = 14.85, \quad \rho_2 = 17.32, \quad \rho_3 = 19.79, \quad \rho_4 = 22.26, \quad \rho_5 = 24.73.$$

Figure 1(c) contains the plot of five periodic orbits  $\bar{\gamma}_i$  ( $i = 1, \dots, 5$ ) at  $\rho = \rho_i$  ( $i = 1, \dots, 5$ ), and the Appendix contains the first 15 Fourier coefficients of  $\bar{\gamma}_1$  and  $\bar{\gamma}_4$ . Table 2 contains the data of the rigorous computation of the Floquet normal forms of the fundamental matrix solutions associated to  $\bar{\gamma}_1$  and  $\bar{\gamma}_4$ . More precisely, it contains the dimension  $m$  of the finite dimensional projection, the computational parameter  $M$  and the enclosing radius  $r$ .

Some of the radii polynomials  $p_k(r)$  built during the rigorous computation of the Floquet normal form of the fundamental matrix solution associated to the periodic orbit  $\bar{\gamma}_4$  are plotted in Figure 3. The bold line on the  $r$ -axis corresponds to the interval

$$INT = [1.794002077820062 \cdot 10^{-10} \quad 0.005654240115476] \tag{58}$$

where all the radii polynomials are negative.

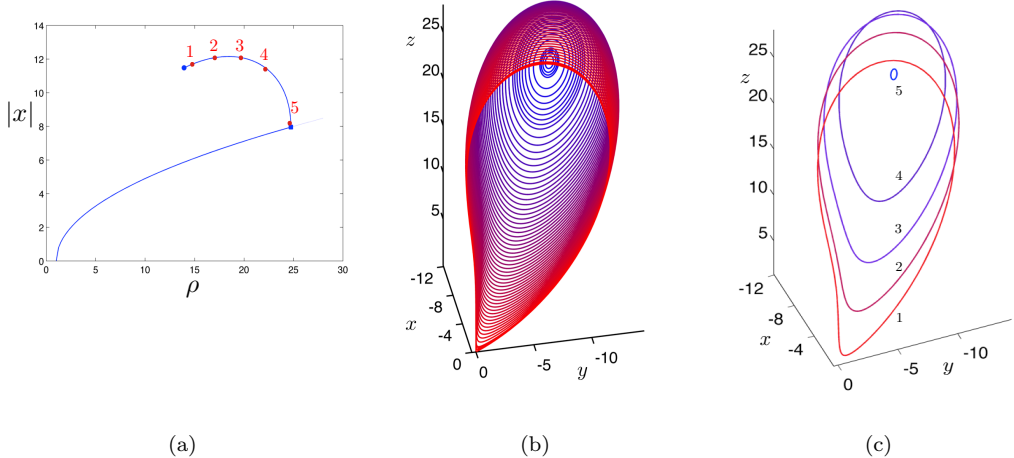


Figure 1: (a) A simple bifurcation diagram for the Lorenz equations (48). The labelled points correspond to the values  $\rho = \rho_i$  ( $i = 1, 2, \dots, 5$ ). (b) Some of the rigorously computed periodic orbits on the branch joining the Hopf bifurcation and the homoclinic point. (c) The periodic solutions corresponding to  $\rho = \rho_i$  ( $i = 1, \dots, 5$ ).

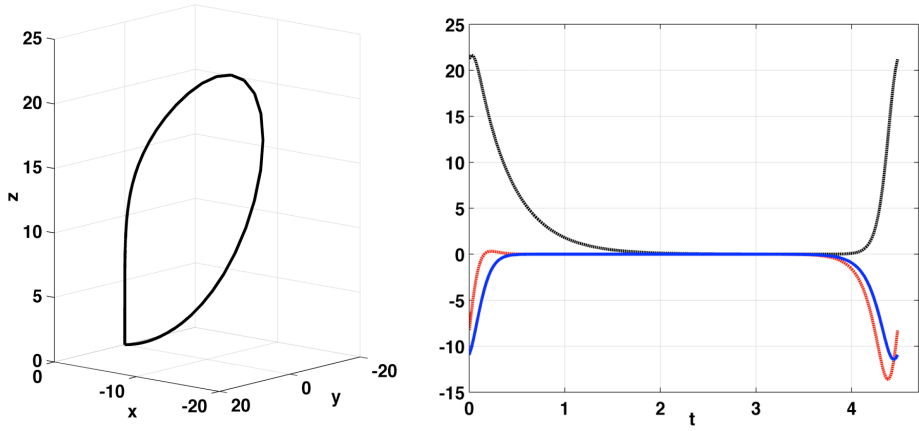


Figure 2: Periodic orbit at  $\rho = 13.927$ . On the left, the orbit is drawn in the state space, while on right the  $x$  (blue),  $y$  (red),  $z$  (black) coordinates are plotted separately as function of time. A genuine solution has been proved to exist with Fourier coefficients in a ball of radius  $r = 1.893591107536733 \cdot 10^{-8}$  around the numerical solution.

| $\rho$ | $\bar{\tau}_\gamma$ | $m_\gamma$ | $r_\gamma$                         |
|--------|---------------------|------------|------------------------------------|
| 24.736 | 0.652859396941149   | 30         | $9.469873202388920 \cdot 10^{-11}$ |
| 24.436 | 0.663384674511011   | 30         | $5.478345151088000 \cdot 10^{-12}$ |
| 23.200 | 0.710825719902523   | 40         | $3.071478394415574 \cdot 10^{-12}$ |
| 20.800 | 0.827536078261055   | 40         | $1.857127168671614 \cdot 10^{-12}$ |
| 16.000 | 1.302497474229172   | 40         | $2.574513942375312 \cdot 10^{-12}$ |
| 15.400 | 1.435095007378964   | 40         | $1.178559327141313 \cdot 10^{-11}$ |
| 14.900 | 1.594009133698383   | 48         | $4.951779335080891 \cdot 10^{-12}$ |
| 14.300 | 1.955959084775736   | 48         | $5.924372707046972 \cdot 10^{-10}$ |
| 14.100 | 2.243447758187898   | 56         | $3.426711644299483 \cdot 10^{-10}$ |
| 14.000 | 2.565212920927481   | 56         | $2.018825516161773 \cdot 10^{-08}$ |
| 13.980 | 2.684270226581966   | 60         | $1.090913664984519 \cdot 10^{-08}$ |
| 13.960 | 2.859882454655782   | 60         | $6.320026130098352 \cdot 10^{-08}$ |
| 13.940 | 3.201446568839638   | 60         | $1.009627398529485 \cdot 10^{-06}$ |
| 13.932 | 3.540414720761810   | 60         | $8.496363668377804 \cdot 10^{-06}$ |
| 13.928 | 4.038292895738813   | 80         | $3.658487332536346 \cdot 10^{-07}$ |
| 13.927 | 4.481359736174591   | 100        | $1.893591107536733 \cdot 10^{-08}$ |

Table 1: Data associated to the computer-assisted proofs of existence (done with the radii polynomials) of several periodic orbits of the Lorenz equations (48) at different parameter values.

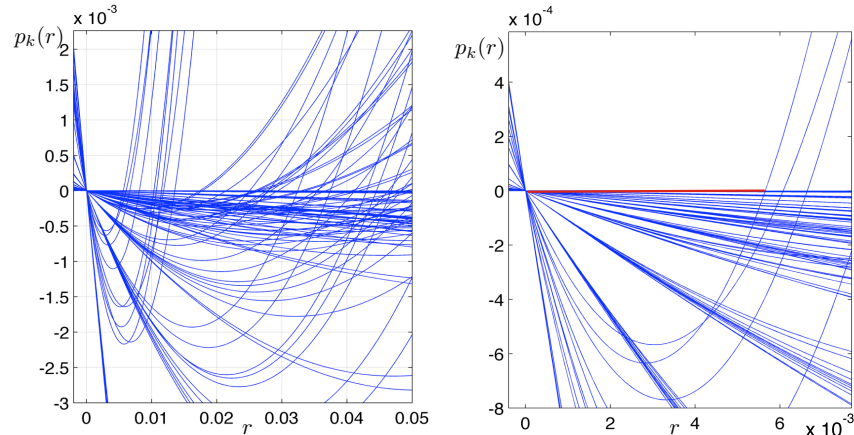


Figure 3: Plot of the radii polynomials  $p_k(r)$  constructed for the rigorous computation of the Floquet normal form of the fundamental matrix solution associated to the periodic solution #4 given by  $\gamma_4$ . On the right: a magnification of the radii polynomials close to  $r = 0$ . The red line denotes the interval  $INT$  given in (58), where all the  $p_k(r)$  are negative.

| # | sol | $\rho$ | $m$ | $M$ | $r$                       |
|---|-----|--------|-----|-----|---------------------------|
| 1 |     | 14.85  | 180 | 900 | $1.734418508431413e - 06$ |
| 2 |     | 17.32  | 90  | 180 | $4.475523531229062e - 09$ |
| 3 |     | 19.79  | 70  | 120 | $3.602266592011710e - 10$ |
| 4 |     | 22.26  | 60  | 100 | $1.794002077820062e - 10$ |
| 5 |     | 24.73  | 40  | 80  | $1.603957178607352e - 09$ |

Table 2: Data associated to the rigorous computation of the Floquet normal form of the fundamental matrix solution for each of the periodic orbit  $\gamma_i$  ( $i = 1, \dots, 5$ ).  $m$  is the dimension of the finite dimensional projection,  $M$  is the computational parameter and  $r$  is the radius of the ball centered at the approximate solution in  $\Omega^s$  within which a genuine solution of (6) exists.

From the rigorous computations of the Floquet normal form, we noticed that the odd Fourier coefficients of  $Q(t)$  are almost vanishing, suggesting that  $Q(t)$  is a  $\tau_\gamma$ -periodic function, rather than  $2\tau_\gamma$ -periodic. This is not in contradiction with Floquet Theorem. In the Appendix, we present the numerical approximation  $\bar{R}$  and the first even Fourier coefficients  $\bar{Q}_k$  for the solutions #1 and #4. Since the Fourier coefficients  $\bar{Q}_k$  corresponding to a periodic orbit *close* to the homoclinic orbit decrease slower, larger values of  $m$  and  $M$  were necessary to obtain successful computations.

We now have all the ingredients necessary to construct the tangent bundles: first we compute the intervals containing the spectrum and the eigenvectors the interval value matrix  $R$ , then, in light of Theorem 3.7, the multiplication of the stable and unstable directions (given by the eigenvectors of  $R$ ) with the function  $Q(\theta)$  yields rigorously the *tube* enclosing the complete stable and unstable bundles. As already mentioned above, the codes necessary to compute the Floquet normal forms for the Lorenz equations can be found in [19].

| Sol # | Center              | Radius                             |
|-------|---------------------|------------------------------------|
| 1     | -15.109380514113965 | $6.535796640191043 \cdot 10^{-6}$  |
|       | 1.442713847447833   | $2.445722953735543 \cdot 10^{-4}$  |
| 2     | -14.418434214853773 | $1.581998979110051 \cdot 10^{-8}$  |
|       | 0.751767548187609   | $2.292988975871850 \cdot 10^{-7}$  |
| 3     | -14.075379469563303 | $1.120430189449109 \cdot 10^{-9}$  |
|       | 0.408712802896790   | $1.443149018164319 \cdot 10^{-8}$  |
| 4     | -13.840311255652775 | $4.525292794068323 \cdot 10^{-10}$ |
|       | 0.173644588986231   | $6.273796862526999 \cdot 10^{-9}$  |
| 5     | -13.667080400789002 | $4.104230777149636 \cdot 10^{-9}$  |
|       | 0.000413734122254   | $9.998501090433916 \cdot 10^{-6}$  |

Table 3: Lyapunov exponents for each of the periodic orbit  $\gamma_i$  ( $i = 1, \dots, 5$ ). For each solution, we report the center and the radius of the interval vectors enclosing the exponents. Note that we could prove the existence of the eigenvectors  $v_j$  associated to  $\mu_j$  within accuracy given by  $r$ .

Table 3 lists the Lyapunov exponents of the periodic orbits, as defined in Definition 3.6, and it also contains the radii of the intervals enclosing the stable and unstable eigen-couple of  $R$  while in Figure 4 the tangent bundles are depicted. In Appendix the complete list of the eigen-decomposition of the interval matrices  $R$  is also provided.

Before closing this section, let us make few remarks. The radii  $r$  of the ball  $B_{\bar{x}}(r)$  showed in Table 2 come as result of different ingredients which are in some sense in competition. First of all the accuracy of the enclosure of the Floquet normal form is limited by the

enclosure of the periodic orbit  $\gamma(t)$ : if  $s = s^*$  one can not expect the radius  $r$  to be smaller than the radius  $r_\gamma$ . Moreover the radius  $r$  of the ball  $B_{\bar{x}}(r)$  in  $\Omega^s$ , where the existence of the genuine solution is proved to exist, depends on how close the numerical approximation is to the real solution. As already said, the definition of the numerical solution  $(\bar{R}, \bar{Q}_k)$  comes from the combination of two numerical integrations, from where we extract  $\mathcal{R}$  and  $\mathcal{Q}_k$ , and the implementation of a Newton scheme to find the zeros of the finite dimensional problem  $f^{(m)} = 0$ . For the first we adopted a variable time step Runge Kutta method of fourth order, as implemented in the built in Matlab function `ode45`, while the Newton scheme is run until  $|f^{(m)}|_\infty < 2 \cdot 10^{-14}$ . Finally, the performance of  $r$  is given by the choice of the finite dimensional parameter  $m$  and the computational parameter  $M$ . While the first addresses a theoretical issue and fixes the dimension of the Galerkin projection, the second serves to better estimate the various bounds necessary in the proof. If on one side a choice of large values for  $m$  and  $M$  decreases the analytical tail errors, on the other side it increases the number of computations and therefore the error propagation and the computational time. Thus the best result is often given as a tradeoff between this two competitors.

## 4.2 The $\zeta^3$ -model: non orientable tangent bundles

It is known that if a Floquet multiplier of a periodic orbit is negative, then the corresponding tangent bundle is not orientable. Moreover, in the case of a saddle periodic orbit of a three-dimensional system, the two non-trivial Floquet multipliers are real and their product is positive. Therefore both the tangent bundles are either orientable or not orientable and, in the latter case, they are topologically equivalent to a Möbius strip, see [16].

An example of a dynamical system with periodic orbits that exhibit this behavior is the so called  $\zeta^3$ -model considered in [17]

$$\begin{cases} \dot{x} = y \\ \dot{y} = z \\ \dot{z} = \alpha x - x^2 - \beta y - z. \end{cases} \quad (59)$$

For  $\beta = 2$ , as  $\alpha$  varies, the periodic orbits of system (59) produce an interesting bifurcation diagram. We refer to [16] and [18] for a detailed analysis of the bifurcation diagram and on the genesis of periodic orbits, called twisted periodic orbits, with non orientable invariant manifolds. We focus on a particular twisted periodic orbit corresponding to  $\alpha = 3.372$  lying on the branch emanating from a period-doubling bifurcation that occurs at  $\alpha \approx 3.125$ .

Following the same procedure as before, we rigorously compute the enclosure of the periodic orbit  $\gamma(t)$  and subsequently the enclosure of the matrix  $R$  and of the matrix function  $Q(t)$ , hence producing an explicit Floquet normal form as in (2). Then, we extract the necessary stability parameters and we recover the stable and unstable tangent bundles using (47). Figure 5 shows the resulting bundles.

For the rigorous computation of the periodic orbit we chose  $m_\gamma = 30$  proving the genuine periodic orbit to live in a ball of radius  $r_\gamma = 1.657473362439634 \cdot 10^{-12}$  around the numerical approximation, ( $s^* = 2$ ), while for the enclosure of the Floquet normal form of the principal fundamental matrix solution of the linearized problem we set  $m = 50$ ,  $M = 100$  yielding the enclosure radius  $r = 8.327055238174269 \cdot 10^{-10}$ . Having computed the intervals enclosing the period  $\tau$  of the orbit and the eigenvalues of  $R$ , we realize that the absolute values of the two nontrivial Floquet multipliers satisfy

$$\begin{aligned} |\sigma_1| &\in [0.007038336031738 \quad 0.007038336266547] \\ |\sigma_2| &\in [1.527362891655825 \quad 1.527363232279426] \end{aligned} .$$

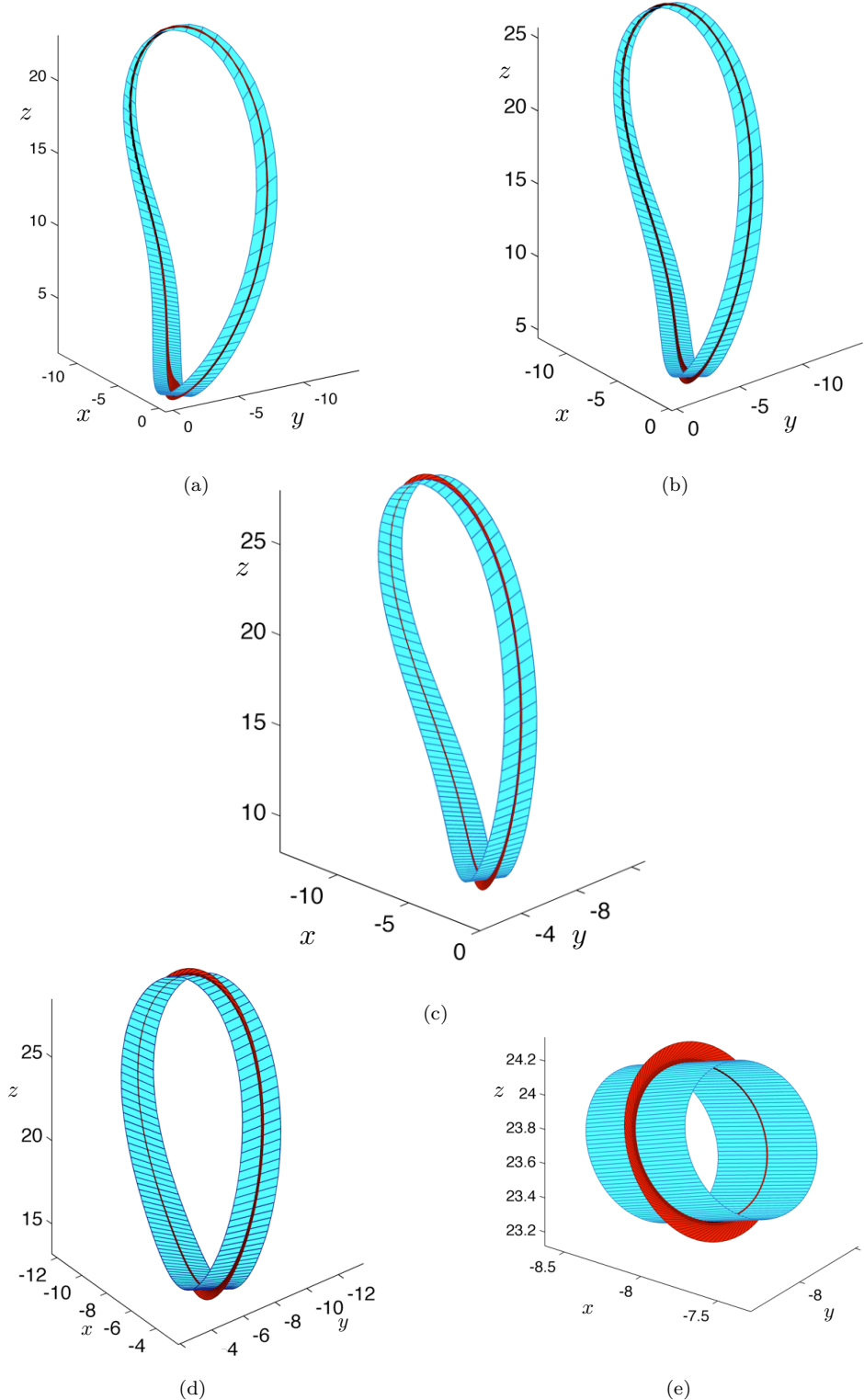
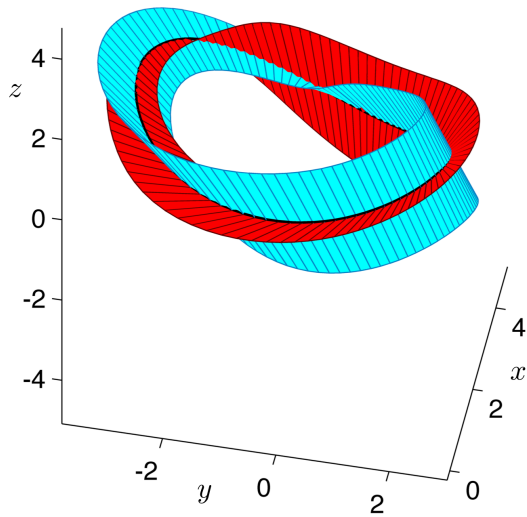
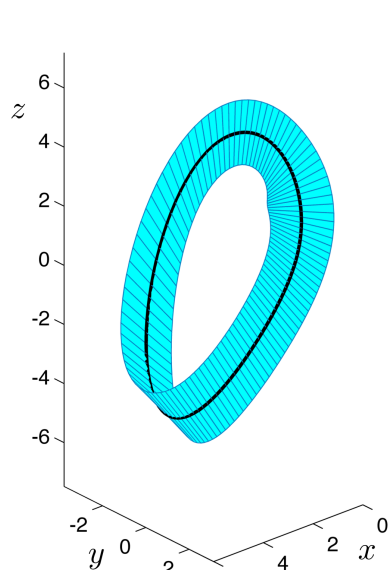


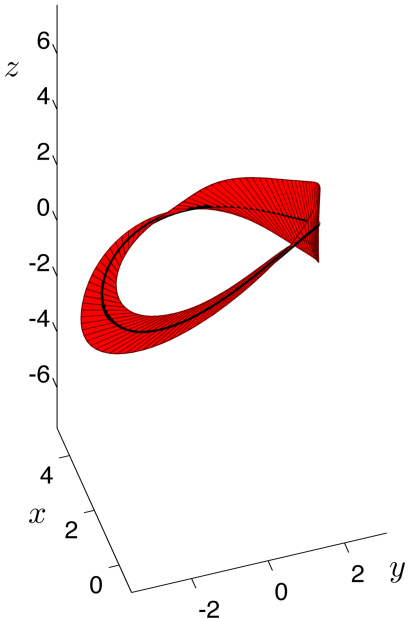
Figure 4: Plot of the tangent stable (turquoise) and unstable (red) bundles of each of the periodic orbits  $\gamma_i$ . Figures (a)-(b)-(c)-(d)-(e) concern respectively  $\gamma_1, \gamma_2, \gamma_3, \gamma_4, \gamma_5$ .



(a)



(b)



(c)

Figure 5: Rigorously computed stable (turquoise) and unstable (red) tangent bundles of a periodic orbit of the  $\zeta^3$  model with negative Floquet multipliers

To conclude we emphasize the role played by the continuous function  $Q(\theta)$  in the construction of the tangent bundles. As proved in Theorem 3.7, as  $\theta$  changes, the eigenvector  $w_j^\theta$  of  $\Phi_\theta(\tau)$  associated to the Floquet multiplier  $\sigma_j$  is given by  $w_j^\theta = Q(\theta)v_j$ , where  $v_j$  is the eigenvector of  $R$  relative to the eigenvalue  $\mu_j$ . The function  $Q(\theta)$  is continuous and  $2\tau$ -periodic, but the tangent bundles are smooth manifolds, therefore the eigenspaces  $E_s^\theta$  and  $E_u^\theta$ , as function of  $\theta \in [0, 2\tau]$ , must be a double covering. That implies that  $w_j^\tau = Q(\tau)v_j$  has to be an eigenvector of  $\Phi(\tau)$  associated to the Floquet multiplier  $\sigma_j$ , i.e.  $\text{span}\{v_j\} = \text{span}\{w_j^\tau\}$ . In the case of the Lorenz equations (48),  $Q(\tau)$  turns to be the identity matrix, therefore the last relation is simply verified. But in case of the  $\zeta^3$ -model and in general when the bundle is not orientable,  $Q(\tau)$  need not be the identity matrix. Indeed, in the considered example,  $Q(\tau)$  results to stay in a small interval around

$$Q = \begin{bmatrix} -1.675372218349393 & -1.030485782114017 & -0.456425794029489 \\ 1.323704549546922 & 1.019713990251906 & 0.894577662024640 \\ 0.970176001842336 & 1.480298639600749 & -0.344341771902499 \end{bmatrix}$$

and the relation  $\text{span}\{v_j\} = \text{span}\{w_j^\tau\}$  still holds.

### 4.3 Recovering of the Floquet multipliers

In this final section, we discuss how to recover a posteriori the Floquet multipliers associated to the periodic orbit  $\gamma(t)$ , that is the eigenvalues of the monodromy matrix  $\Phi_\theta(\tau)$ . First recall from Lemma 3.3 that the Floquet multipliers, denoted by  $\sigma_j$ , are independent of  $\theta$  and from Theorem 3.7 that they solve the equation

$$\Phi_\theta(\tau)w_j^\theta = \sigma_j w_j^\theta \quad (60)$$

for any  $\theta$ . In the proof of Theorem 3.7 we realized that  $\sigma_j^2 = e^{\mu_j 2\tau}$  where  $\mu_j$  are the eigenvalues of the matrix  $R$ . Thus the Floquet multipliers are known up to a sign, i.e.  $\sigma_j = \pm e^{\mu_j \tau}$ . Therefore, by choosing  $\theta = 0$  in (60), it is enough to check whether  $\Phi(\tau)w_j^0$  is equal to  $+e^{\mu_j \tau}w_j^0$  or to  $-e^{\mu_j \tau}w_j^0$ . Recall that the Floquet normal form  $\Phi(t) = Q(t)e^{Rt}$  satisfies  $Q(0) = I$  and recall from (47) that  $w_j^\theta \stackrel{\text{def}}{=} Q(\theta)v_j$ . Hence, since  $(\mu_j, v_j) \in \Sigma(R)$ , one has that  $\Phi(\tau)w_j^0 = Q(\tau)e^{R\tau}v_j = Q(\tau)e^{\mu_j \tau}v_j$ . Thus it reduces to compute the vectors  $Q(\tau)e^{\mu_j \tau}v_j$  and  $e^{\mu_j \tau}v_j$  and to compare them.

Having computed the enclosure of  $Q(t)$  in terms of the Fourier coefficients and the bounds for  $\mu_j$  and  $v_j$ , denote by  $\mathcal{I}_{\sigma_j}$  the interval enclosing  $Q(\tau)e^{\mu_j \tau}v_j$  and by  $\mathcal{I}_j^+$ ,  $\mathcal{I}_j^-$  the intervals enclosing  $e^{\mu_j \tau}v_j$  and  $-e^{\mu_j \tau}v_j$ , respectively. The sign of the Floquet multiplier  $\sigma_j$  is determined if  $\mathcal{I}_{\sigma_j}$  intersects only one of the intervals  $\mathcal{I}_j^+$  and  $\mathcal{I}_j^-$ , while no conclusion can be achieved if  $\mathcal{I}_{\sigma_j}$  is so large to intersect both of them. Note that  $\mathcal{I}_{\sigma_j}$  has to intersect at least one  $\mathcal{I}_j^\pm$ . The choice  $\theta = 0$  in (60) increases the chances of successfully recovering the Floquet multipliers since in this case, the computation of the matrix exponentiation  $e^{R\tau}$ , a computation that can dramatically increase the error propagation, can be avoided.

Finally, Table 4 and Table 5 contain the intervals  $\mathcal{I}_{\sigma_j}$  and  $\mathcal{I}_j^\pm$ ,  $j = 1, 2$  associated to the solution #3 of the Lorenz equations and of the solution of the  $\zeta^3$ -model. That shows that the Floquet multipliers  $\sigma_1, \sigma_2$  are both positive for the periodic solution of the Lorenz equations and are both negative for the periodic solution the  $\zeta^3$ -model.

Solution Lorenz #3

$$|\sigma_2| \in [0.359965418958973 \ 0.359965419696942] \cdot 10^{-5}$$

$$|\sigma_1| \in [1.439037708132836 \ 1.439037745123575]$$

| $\mathcal{I}_{\sigma_1}$  | $\mathcal{I}_1^+$   |
|---|---|
| $10^{-5}.$  | $10^{-5}.$  |
| $\begin{bmatrix} 0.275643268865818 & 0.275643271985182 \\ 0.065076919481043 & 0.065076922168721 \\ 0.222173095329639 & 0.222173098339382 \end{bmatrix}$       | $\begin{bmatrix} 0.275643269739635 & 0.275643271111366 \\ 0.065076920354861 & 0.065076921294908 \\ 0.222173096203459 & 0.222173097465571 \end{bmatrix}$       |
| $\mathcal{I}_{\sigma_2}$  | $\mathcal{I}_2^+$   |
| $\begin{bmatrix} -0.263299353291831 & -0.263299298199846 \\ -1.237252678484705 & -1.237252598357060 \\ -0.686082354892901 & -0.686082288933197 \end{bmatrix}$ | $\begin{bmatrix} -0.263299349897387 & -0.263299301594310 \\ -1.237252675090274 & -1.237252601751541 \\ -0.686082351498413 & -0.686082292327618 \end{bmatrix}$ |

Table 4: Interval vectors  $\mathcal{I}_{\sigma_j}$  and  $\mathcal{I}_j^+$ ,  $j = 1, 2$  associated to sol#3 for the Lorenz equations (48). It holds  $\mathcal{I}_j^+ \subset \mathcal{I}_{\sigma_j}$ ,  $j = 1, 2$  proving that the Floquet multipliers are positive

Solution  $\zeta^3$ -model

$$|\sigma_1| \in [0.007038336031738 \ 0.007038336266547]$$

$$|\sigma_2| \in [1.527362891655825 \ 1.527363232279426]$$

| $\mathcal{I}_{\sigma_1}$  | $\mathcal{I}_1^+$   |
|---|---|
| $\begin{bmatrix} 0.001505025554611 & 0.001505026041576 \\ 0.001935764317690 & 0.001935764886660 \\ -0.006597415507817 & -0.006597415070914 \end{bmatrix}$   | $\begin{bmatrix} -0.001505025849095 & -0.001505025747089 \\ -0.001935764660362 & -0.001935764543986 \\ 0.006597415153419 & 0.006597415425314 \end{bmatrix}$ |
| $\mathcal{I}_{\sigma_2}$  | $\mathcal{I}_2^+$   |
| $\begin{bmatrix} 0.995820356220745 & 0.995821132336306 \\ -0.143670022815996 & -0.143669207167412 \\ -1.149146933067294 & -1.149146355489062 \end{bmatrix}$ | $\begin{bmatrix} -0.995820892892411 & -0.995820595664657 \\ 0.143669561398723 & 0.143669668584703 \\ 1.149146478567386 & 1.149146809988988 \end{bmatrix}$   |

Table 5: Interval vectors  $\mathcal{I}_{\sigma_j}$  and  $\mathcal{I}_j^+$ ,  $j = 1, 2$  associated to solution of the  $\zeta^3$ -model. It holds  $-\mathcal{I}_j^+ = \mathcal{I}_j^- \subset \mathcal{I}_{\sigma_j}$ ,  $j = 1, 2$  proving that the Floquet multipliers are negative.

## 5 Acknowledgments

We would like to thank Marcio Gameiro and Jason D. Mireles James for helpful discussions.

## 6 Appendix

The period and the Fourier coefficients of  $\bar{\gamma}_1$  and  $\bar{\gamma}_4$ :

Solution # 1

$$\bar{\tau}_\gamma = 1.614093492553360, \quad \bar{\xi}_0 = \begin{bmatrix} -2.780059260523741 \\ -2.780059260523741 \\ 7.947403837193834 \end{bmatrix}$$

| $\bar{\xi}_1$                             | $\bar{\xi}_2$                              | $\bar{\xi}_3$                             |
|---|--|---|
| $-2.103424940338396 - 0.563375873719758i$ | $-1.148118935964748 - 0.463407706727962i$  | $-0.549947197921830 - 0.250386371164224i$ |
| $-1.884119489414622 - 1.382176565306859i$ | $-0.787337295052375 - 1.357264730825950i$  | $-0.257543323733286 - 0.892620573144838i$ |
| $3.500814040190368 - 2.277378948991177i$  | $1.714800528134896 - 0.931203853246065i$   | $0.934628045117667 - 0.303909720680586i$  |
| $\bar{\xi}_4$                             | $\bar{\xi}_5$                              | $\bar{\xi}_6$                             |
| $-0.245788932283429 - 0.120107696132124i$ | $-0.105336849992997 - 0.056272958254793i$  | $-0.044023808302604 - 0.026405465627272i$ |
| $-0.058771534568073 - 0.502820944185082i$ | $0.004190084515215 - 0.261295452687129i$   | $0.017649360354828 - 0.129228411176272i$  |
| $0.498026421896317 - 0.069036329230910i$  | $0.255207598883747 + 0.004096081252986i$   | $0.126183314309363 + 0.019020106397201i$  |
| $\bar{\xi}_7$                             | $\bar{\xi}_8$                              | $\bar{\xi}_9$                             |
| $-0.018110918227797 - 0.012412554201161i$ | $-0.007364503589650 - 0.005817610383848i$  | $-0.002963317111988 - 0.002709075113557i$ |
| $0.015711945800080 - 0.061762842200829i$  | $0.010752476253377 - 0.028751865908767i$   | $0.006527743303825 - 0.013090855079841i$  |
| $0.060511917346837 + 0.016657990661909i$  | $0.028266369399563 + 0.011223417581133i$   | $0.012901208489663 + 0.006732467383552i$  |
| $\bar{\xi}_{10}$                          | $\bar{\xi}_{11}$                           | $\bar{\xi}_{12}$                          |
| $-0.001179210881516 - 0.001251358716240i$ | $-0.000463309508391 - 0.000573118774730i$  | $-0.000179268598732 - 0.000260306136273i$ |
| $0.003691955959910 - 0.005841675521921i$  | $0.001990769285304 - 0.002556997317175i$   | $0.001036684527908 - 0.001097713261045i$  |
| $0.005764884939599 + 0.003774872882279i$  | $0.00252460767658795 + 0.002023019415141i$ | $0.001083619790267 + 0.00104891330054i$   |
| $\bar{\xi}_{13}$                          | $\bar{\xi}_{14}$                           | $\bar{\xi}_{15}$                          |
| $-0.000068057085571 - 0.000117293446836i$ | $-0.000025210012126 - 0.000052457038185i$  | $-0.000009032463269 - 0.000023294288074i$ |
| $0.000525507912207 - 0.000461697204554i$  | $0.000260669467808 - 0.000189846136106i$   | $0.000126984126766 - 0.000076035322684i$  |
| $0.000455456453909 + 0.000530056624236i$  | $0.000187064896143 + 0.000262329087681i$   | $0.000074796643384 + 0.00012754811379i$   |
| <hr/>                                     |  |   |

| $\bar{\xi}_1$                              | $\bar{\xi}_2$                               | $\bar{\xi}_3$                               |
|--|---|---|
| $-1.957527201575398 - 0.358818882759485i$  | $-0.335512945846433 - 0.016213444633248i$   | $-0.047773518005275 + 0.003264331987478i$   |
| $-1.657745833247766 - 1.994268440246074i$  | $-0.308421346986976 - 0.576833494637121i$   | $-0.055955243858351 - 0.116475274417622i$   |
| $2.644506821861307 - 2.227265633430878i$   | $0.566785859807531 - 0.332890753309569i$    | $0.114165757724204 - 0.053764689555239i$    |
| $\bar{\xi}_4$                              | $\bar{\xi}_5$                               | $\bar{\xi}_6$                               |
| $-0.006558770971049 + 0.000929180341579i$  | $-0.000901308891171 - 0.000177163318124i$   | $-0.000124174690936 + 0.000030576566572i$   |
| $-0.009663969360603 - 0.020989368884455i$  | $-0.001641379501671 - 0.003587906270789i$   | $-0.000277448981776 - 0.000591886640616i$   |
| $0.020940359140456 - 0.009162879791036i$   | $0.003602280657498 - 0.001579182778059i$    | $0.00059485613762 - 0.000270108958042i$     |
| $\bar{\xi}_7$                              | $\bar{\xi}_8$                               | $\bar{\xi}_9$                               |
| $-0.000017112175371 + 0.000005045265812i$  | $-0.0000002356075416 + 0.000000809468453i$  | $-0.0000000323960977 + 0.000000127320510i$  |
| $-0.000046618250245 - 0.000095031349885i$  | $-0.000007766349449 - 0.000014937919344i$   | $-0.0000001281309839 - 0.0000002308608107i$ |
| $0.000095408145471 - 0.000045683567994i$   | $0.000014990676622 - 0.000007640211987i$    | $0.0000002316321304 - 0.0000001263950355i$  |
| $\bar{\xi}_{10}$                           | $\bar{\xi}_{11}$                            | $\bar{\xi}_{12}$                            |
| $-0.000000044474813 + 0.000000019730387i$  | $-0.000000006094973 + 0.000000003022158i$   | $-0.000000000833662 + 0.00000000458564i$    |
| $-0.000000209315706 - 0.000000351842042i$  | $-0.0000000033869024 - 0.0000000052991484i$ | $-0.0000000005431044 - 0.0000000007899402i$ |
| $0.0000000352995514 - 0.0000000206922202i$ | $0.0000000053164861 - 0.0000000033539827i$  | $0.000000007925411 - 0.0000000005385894i$   |
| $\bar{\xi}_{13}$                           | $\bar{\xi}_{14}$                            | $\bar{\xi}_{15}$                            |
| $-0.000000000113788 + 0.00000000069034i$   | $-0.0000000000015496 + 0.00000000010323i$   | $-0.000000000002105 + 0.000000000001535i$   |
| $-0.000000000863573 - 0.0000000001166826i$ | $-0.0000000000136241 - 0.000000000170926i$  | $-0.0000000000021338 - 0.0000000000024847i$ |
| $0.0000000001170712 - 0.000000000857397i$  | $0.0000000000171505 - 0.000000000135398i$   | $0.0000000000024933 - 0.0000000000021224i$  |

Numerical approximation  $\bar{R}$  and even Fourier coefficients  $\bar{Q}_k$ :

Solution # 1

$$\bar{R} = \begin{bmatrix} -1.387511870700525 & 10.413957598738442 & -24.345293393676652 \\ 34.433483055001410 & 16.747540413772924 & -64.490466526574409 \\ 5.910150213980192 & 10.264994080118939 & -29.026695209740538 \end{bmatrix}$$

$$\bar{Q}_0 = \begin{bmatrix} 1.164908177280166 & -1.803172340423295 & 3.576351013779620 \\ -3.091997467130629 & 0.061210130102117 & 1.988125340690924 \\ 2.718036482444605 & 0.825898407183530 & -3.885210588070526 \end{bmatrix}$$

$$\bar{Q}_2 =$$

$$\begin{aligned}
& \left[ \begin{array}{l} -0.866294000482876 - 1.517174563626462i \\ 0.509788425938065 - 0.714866339135450i \\ 0.402372709747515 - 0.063751212963967i \end{array} \right] \quad \left[ \begin{array}{l} 0.138024745785573 + 0.218099611198252i \\ -0.287829114159326 - 0.633681030790011i \\ 0.203769059852901 + 0.107721913625062i \end{array} \right] \quad \left[ \begin{array}{l} 0.321523051493223 + 0.301224125958044i \\ 0.489880443422970 + 1.839100806447159i \\ -0.537890180980384 + 0.144035347276835i \end{array} \right] \\
& \bar{Q}_4 = \\
& \left[ \begin{array}{l} 0.002921350244971 - 0.041026859510501i \\ 0.661612810285463 - 0.36208143572158i \\ -0.220722332917557 + 0.515436548133675i \end{array} \right] \quad \left[ \begin{array}{l} 0.284838788861365 - 0.102407807177850i \\ 0.230422023359519 - 0.053897172370139i \\ -0.015454270152731 + 0.317283993327913i \end{array} \right] \quad \left[ \begin{array}{l} -0.598366228696386 + 0.039927158582337i \\ -0.736642472712952 + 0.218493323289657i \\ 0.382525265190417 - 0.772796160555542i \end{array} \right] \\
& \bar{Q}_6 = \\
& \left[ \begin{array}{l} 0.272254735540097 + 0.193108273854690i \\ 0.346206488506330 + 0.232974541129058i \\ -0.415259741322708 + 0.376758862585817i \end{array} \right] \quad \left[ \begin{array}{l} 0.200555829088783 - 0.035698340068769i \\ 0.247951861450867 + 0.116888303230541i \\ -0.130242646049827 + 0.256517250203223i \end{array} \right] \quad \left[ \begin{array}{l} -0.597856635403175 - 0.217185503512216i \\ -0.565050894702496 - 0.524858613861323i \\ 0.697655874103223 - 0.593956538793055i \end{array} \right] \\
& \bar{Q}_8 = \\
& \left[ \begin{array}{l} 0.226805195194691 + 0.164436218751750i \\ 0.132624286729287 + 0.362338337115273i \\ -0.396602815786101 + 0.163955300090018i \end{array} \right] \quad \left[ \begin{array}{l} 0.127848789361473 - 0.002657587081552i \\ 0.153471968526916 + 0.148905166236442i \\ -0.150058149361482 + 0.153653073255694i \end{array} \right] \quad \left[ \begin{array}{l} -0.417753912756603 - 0.208768292791024i \\ -0.256749954059345 - 0.636445460226098i \\ 0.667238511937733 - 0.280824220397952i \end{array} \right] \\
& \bar{Q}_{10} = \\
& \left[ \begin{array}{l} 0.139141286867885 + 0.105392333409777i \\ 0.022491378705591 + 0.297244131793740i \\ -0.295670715198465 + 0.034690679906638i \end{array} \right] \quad \left[ \begin{array}{l} 0.073450746075024 + 0.005413998475731i \\ 0.07875864111050 + 0.123065445235988i \\ -0.121731432613219 + 0.077394507215750i \end{array} \right] \quad \left[ \begin{array}{l} -0.245560436837712 - 0.140410932437067i \\ -0.071921501008139 - 0.502287082721128i \\ 0.498006841524345 - 0.080182881735437i \end{array} \right] \\
& \bar{Q}_{12} = \\
& \left[ \begin{array}{l} 0.074574329861185 + 0.061221963277495i \\ -0.021085752655787 + 0.197514892292071i \\ -0.191963300440361 - 0.018713774729379i \end{array} \right] \quad \left[ \begin{array}{l} 0.039089264765640 + 0.005851913643466i \\ 0.034950837558746 + 0.084663275771703i \\ -0.083514110368357 + 0.033519476548476i \end{array} \right] \quad \left[ \begin{array}{l} -0.130148022379516 - 0.083821935619066i \\ 0.009763089761531 - 0.331276984497606i \\ 0.323798241079228 + 0.009713985079557i \end{array} \right] \\
& \bar{Q}_{14} = \\
& \left[ \begin{array}{l} 0.036973044527057 + 0.033903826569238i \\ -0.030689170867607 + 0.117291019360528i \\ -0.113726808259459 - 0.031164706653101i \end{array} \right] \quad \left[ \begin{array}{l} 0.019751905247220 + 0.004450594969025i \\ 0.012928757340301 + 0.052434619076431i \\ -0.051799471311031 + 0.011931226793130i \end{array} \right] \quad \left[ \begin{array}{l} -0.064567903024736 - 0.047344137089248i \\ 0.034466100020053 - 0.197102241654019i \\ 0.192411484019366 + 0.036313805087712i \end{array} \right] \\
& \text{Solution # 4} \\
& \bar{R} = \left[ \begin{array}{ccc} -10.355025789684301 & 5.074347263132815 & -4.639314258829991 \\ 0.899060859561549 & 1.009663080648024 & -1.282544953856572 \\ -7.222497813952203 & 4.473311681603017 & -4.32130957630427 \end{array} \right] \\
& \bar{Q}_0 = \left[ \begin{array}{ccc} 1.023958718010556 & -0.675126514730723 & 0.660211296603439 \\ -0.573888622357730 & 0.071633755972287 & -0.013544689908735 \\ 0.593641003024321 & 0.040742151766272 & -0.119448524191943 \end{array} \right] \\
& \bar{Q}_2 = \\
& \left[ \begin{array}{l} -0.047826742741476 - 0.090749687879213i \\ 0.265817278059553 + 0.091999384890591i \\ -0.193372062784211 + 0.147055239961529i \end{array} \right] \quad \left[ \begin{array}{l} 0.252122278258324 - 0.09822333446528i \\ 0.232785054596794 - 0.028752909644381i \\ 0.030279421996656 + 0.406013396545621i \end{array} \right] \quad \left[ \begin{array}{l} -0.229330080277529 - 0.190468845464143i \\ 0.018753383934223 - 0.245059986851624i \\ 0.347429574659487 - 0.063287598335153i \end{array} \right] \\
& \bar{Q}_4 = \\
& \left[ \begin{array}{l} 0.025498974224084 + 0.025507226852369i \\ 0.019926879914556 + 0.060459834467346i \\ -0.074073542381906 + 0.029861690000861i \end{array} \right] \quad \left[ \begin{array}{l} 0.069941219836411 - 0.066317758714468i \\ 0.165349054957407 + 0.041485865858316i \\ -0.030387995391957 + 0.166042842829839i \end{array} \right] \quad \left[ \begin{array}{l} -0.079148400827483 - 0.034227312899873i \\ -0.008554435269462 - 0.155016472536096i \\ 0.151663950249043 - 0.013807569732756i \end{array} \right] \\
& \bar{Q}_6 = \\
& \left[ \begin{array}{l} 0.008288011670258 + 0.004860383652844i \\ 0.001396115699013 + 0.022890324353531i \\ -0.022097257512586 + 0.002295893083263i \end{array} \right] \quad \left[ \begin{array}{l} 0.012918990885743 - 0.015956351350131i \\ 0.050549397456237 + 0.014972378771104i \\ -0.015042801858593 + 0.048889031118857i \end{array} \right] \quad \left[ \begin{array}{l} -0.017599087865688 - 0.005156624049461i \\ -0.002571405701545 - 0.047247077238629i \\ 0.046172957869546 - 0.001868328256481i \end{array} \right] \\
& \bar{Q}_8 = \\
& \left[ \begin{array}{l} 0.001688790296409 + 0.000787492845468i \\ -0.000094100471388 + 0.005833802350177i \\ -0.005671743885677 - 0.000185380438099i \end{array} \right] \quad \left[ \begin{array}{l} 0.002170111882739 - 0.003127608490179i \\ 0.012210251990343 + 0.003899231753956i \\ -0.004112500955533 + 0.011989324632692i \end{array} \right] \quad \left[ \begin{array}{l} -0.003326338289578 - 0.000691224227202i \\ -0.000640755524250 - 0.011472922761902i \\ 0.011377894614169 - 0.000404535129055i \end{array} \right] \\
& \bar{Q}_{10} = \\
& \left[ \begin{array}{l} 0.000307654059622 + 0.000124254364919i \\ -0.000076757144186 + 0.001291949037968i \\ -0.001279612235996 - 0.00012271912113i \end{array} \right] \quad \left[ \begin{array}{l} 0.000347668081985 - 0.000564475242089i \\ 0.002635543312150 + 0.000855548446007i \\ -0.000896750134065 + 0.002613762734525i \end{array} \right] \quad \left[ \begin{array}{l} -0.000584230091926 - 0.000085754177866i \\ -0.000160862924263 - 0.002474471286528i \\ 0.002470710144145 - 0.000120863512284i \end{array} \right] \\
& \bar{Q}_{12} = 1.0e - 03* \\
& \left[ \begin{array}{l} 0.053293732076546 + 0.018836962984192i \\ -0.020444526584427 + 0.264463962191678i \\ -0.263658578699069 - 0.024245634946039i \end{array} \right] \quad \left[ \begin{array}{l} 0.053627551296946 - 0.097323410654047i \\ 0.529941590955565 + 0.167063705717098i \\ -0.173355701294813 + 0.527451834570075i \end{array} \right] \quad \left[ \begin{array}{l} -0.098376036926625 - 0.009320506671707i \\ -0.040745513201438 - 0.494689375231222i \\ 0.494802425816997 - 0.034778433874860i \end{array} \right] \\
& \bar{Q}_{14} = 1.0e - 03* \\
& \left[ \begin{array}{l} 0.008925530239504 + 0.002730948596921i \\ -0.003951084971026 + 0.05179892292212i \\ -0.051092194502835 - 0.004493128366171i \end{array} \right] \quad \left[ \begin{array}{l} 0.008007810390487 - 0.016262173402608i \\ 0.101255843144903 + 0.029979048738808i \\ -0.030934399104456 + 0.100900542958549i \end{array} \right] \quad \left[ \begin{array}{l} -0.016084694725868 - 0.000747676030797i \\ -0.009929269848351 - 0.093673490358287i \\ 0.093718090923293 - 0.009025243987087i \end{array} \right]
\end{aligned}$$

Enclosure of the spectrum and eigenvectors of  $R$ :

Solution # 1

|                  | <i>Stable</i>                   | <i>Unstable</i>                   |
|------------------|---------------------------------|-----------------------------------|
| <i>E.values</i>  | -15.109380514113965             | -1.9711376476 · 10 <sup>-12</sup> |
| <i>E.vectors</i> | -0.751214982423802              | 0.254365252143146                 |
| <i>Rad</i>       | 6.5357966401 · 10 <sup>-6</sup> | 2.4292063094 · 10 <sup>-4</sup>   |
|                  |                                 | 2.4457229537 · 10 <sup>-4</sup>   |

| Solution # 2 |  |   |   |
|--------------|--|---|---|
|              | Stable   |   | Unstable  |
| E.values     | -14.418434214853773  | $-6.3095429563 \cdot 10^{-13}$                              | 0.751767548187609   |
| E.vectors    | -0.749706208066872<br>-0.289601764001737<br>-0.595039007018088 | 0.206834663675313<br>0.877249310542877<br>0.433189414753372 | 0.230648743314282<br>0.889680889496459<br>0.394041967399836 |
| Rad          | $1.5819989791 \cdot 10^{-8}$                                   | $2.2544294848 \cdot 10^{-7}$                                | $2.2929889758 \cdot 10^{-7}$                                |

| Solution # 3 |  |   |   |
|--------------|--|---|---|
|              | Stable                                   |   | Unstable                                |
| E.values     | -14.075379469563303<br>0.765749307086543 | $-1.9608231416 \cdot 10^{-13}$<br>0.150573371977808 | 0.408712802896790<br>-0.182969022197064 |
| E.vectors    | 0.180786590407435<br>0.617206778499179   | 0.836967739109956<br>0.526129892080275              | -0.85977763658707<br>-0.476764652668675 |
| Rad          | $1.1204301894 \cdot 10^{-9}$             | $1.4128237162 \cdot 10^{-8}$                        | $1.4431490181 \cdot 10^{-8}$            |

| Solution # 4 |  |   |  |
|--------------|--|---|--|
|              | Stable                                   |   | Unstable                                 |
| E.values     | -13.840311255652775<br>0.797501959393221 | $-1.4330029932 \cdot 10^{-13}$<br>0.078973004231439 | 0.173644588986231<br>-0.117842783974500  |
| E.vectors    | 0.003822364878423<br>0.603304246869447   | 0.755631456467173<br>0.650218706744094              | -0.792087449202407<br>-0.598924495309018 |
| Rad          | $4.5252927940 \cdot 10^{-10}$            | $6.1203260279 \cdot 10^{-9}$                        | $6.2737968625 \cdot 10^{-9}$             |

| Solution # 5 |   |  |  |
|--------------|---|--|--|
|              | Stable                                    |  | Unstable                               |
| E.values     | -13.667080400789002<br>-0.863856794412098 | $9.0011809244 \cdot 10^{-14}$<br>0.232602509848306 | 0.000413734122254<br>0.287469286236642 |
| E.vectors    | 0.300568560001125<br>-0.404240002333891   | 0.819824988052658<br>0.523242832131249             | 0.854693879140621<br>0.432272810190687 |
| Rad          | $4.1042307771 \cdot 10^{-9}$              | $1.0966119731 \cdot 10^{-5}$                       | $9.9985010904 \cdot 10^{-6}$           |

## References

- [1] G. Floquet. Sur les équations différentielles linéaires à coefficients périodiques. *Ann. Sci. École Norm. Sup. (2)*, 12:47–88, 1883.
- [2] Carmen Chicone. *Ordinary differential equations with applications*, volume 34 of *Texts in Applied Mathematics*. Springer, New York, second edition, 2006.
- [3] X. Cabré, E. Fontich, and R. de la Llave. The parameterization method for invariant manifolds. III. Overview and applications. *J. Differential Equations*, 218(2):444–515, 2005.
- [4] Piotr Zgliczynski.  $C^1$  Lohner algorithm. *Found. Comput. Math.*, 2(4):429–465, 2002.
- [5] Tomasz Kapela and Carles Simó. Computer assisted proofs for nonsymmetric planar choreographies and for stability of the Eight. *Nonlinearity*, 20(5):1241–1255, 2007.
- [6] A. Haro and R. de la Llave. A parameterization method for the computation of invariant tori and their whiskers in quasi-periodic maps: explorations and mechanisms for the breakdown of hyperbolicity. *SIAM J. Appl. Dyn. Syst.*, 6(1):142–207 (electronic), 2007.
- [7] À. Haro and R. de la Llave. A parameterization method for the computation of invariant tori and their whiskers in quasi-periodic maps: numerical algorithms. *Discrete Contin. Dyn. Syst. Ser. B*, 6(6):1261–1300 (electronic), 2006.
- [8] A. Haro and R. de la Llave. A parameterization method for the computation of invariant tori and their whiskers in quasi-periodic maps: rigorous results. *J. Differential Equations*, 228(2):530–579, 2006.
- [9] Sarah Day, J.-P. Lessard, and Konstantin Mischaikow. Validated continuation for equilibria of PDEs. *SIAM J. Numer. Anal.*, 45(4):1398–1424 (electronic), 2007.

- [10] Marcio Gameiro and J.-P. Lessard. Analytic estimates and rigorous continuation for equilibria of higher-dimensional PDEs. *J. Differential Equations*, 249(9):2237–2268, 2010.
- [11] Richard S. Varga. On diagonal dominance arguments for bounding  $\|A^{-1}\|_\infty$ . *Linear Algebra and its Applications*, 14(3):211–217, 1976.
- [12] Alexandre Goldsztejn. On the exponentiation of interval matrices. Preprint, 2009.
- [13] Edward P. Oppenheimer and Anthony N. Michel. Application of interval analysis techniques to linear systems. II. The interval matrix exponential function. *IEEE Trans. Circuits and Systems*, 35(10):1230–1242, 1988.
- [14] R. Castelli and J.-P. Lessard. A method to rigorously enclose eigendecompositions of interval matrices. *Submitted*.
- [15] S.M. Rump. INTLAB - INTerval LABoratory. In Tibor Csendes, editor, *Developments in Reliable Computing*, pages 77–104. Kluwer Academic Publishers, Dordrecht, 1999. <http://www.ti3.tu-harburg.de/rump/>.
- [16] Hinke M. Osinga. Nonorientable manifolds in three-dimensional vector fields. *Internat. J. Bifur. Chaos Appl. Sci. Engrg.*, 13(3):553–570, 2003.
- [17] A. Arneodo, P. H. Coullet, E. A. Spiegel, and C. Tresser. Asymptotic chaos. *Phys. D*, 14(3):327–347, 1985.
- [18] Mark E. Johnson, Michael S. Jolly, and Ioannis G. Kevrekidis. Two-dimensional invariant manifolds and global bifurcations: some approximation and visualization studies. *Numer. Algorithms*, 14(1-3):125–140, 1997. Dynamical numerical analysis (Atlanta, GA, 1995).
- [19] R. Castelli and J.-P. Lessard. Rigorous numerics in Floquet theory: computing stable and unstable bundles of periodic orbits; INTLAB Codes, <http://www.math.rutgers.edu/~lessard/floquet>